UHECR2022: 6TH INTERNATIONAL SYMPOSIUM ON ULTRA HIGH ENERGY COSMIC RAYS

6th October 2022

GSSI, L'Aquila, Italy

Interpreting the cosmic ray spectrum and composition measurements across the ankle and up to the highest energies with the data of the Pierre Auger Observatory

Eleonora Guido*,
on behalf of the Pierre Auger Collaboration

*Universität Siegen, Siegen, Germany

Introduction

Combined fit of the Pierre Auger Observatory measurements (spectrum and composition) *at ultra-high-energy* (UHE)

- Combined fit above $10^{18.7}$ eV (above the ankle) already published[1]

  → extension to low energies to include the ankle feature

- **Preliminary results already shown at ICRC2021**[2]
- Paper by the Pierre Auger Collaboration **to be soon submitted to a journal**

[1] The Pierre Auger Collaboration, JCAP04 (2017) 038
[2] E. Guido for the Pierre Auger Collaboration PoS(ICRC2021)311

Measurements of the energy and mass composition

Surface Detector (SD)

- Duty cycle: ~100%
- Measurement of the lateral distribution of signals

Hybrid events = observed by both detectors

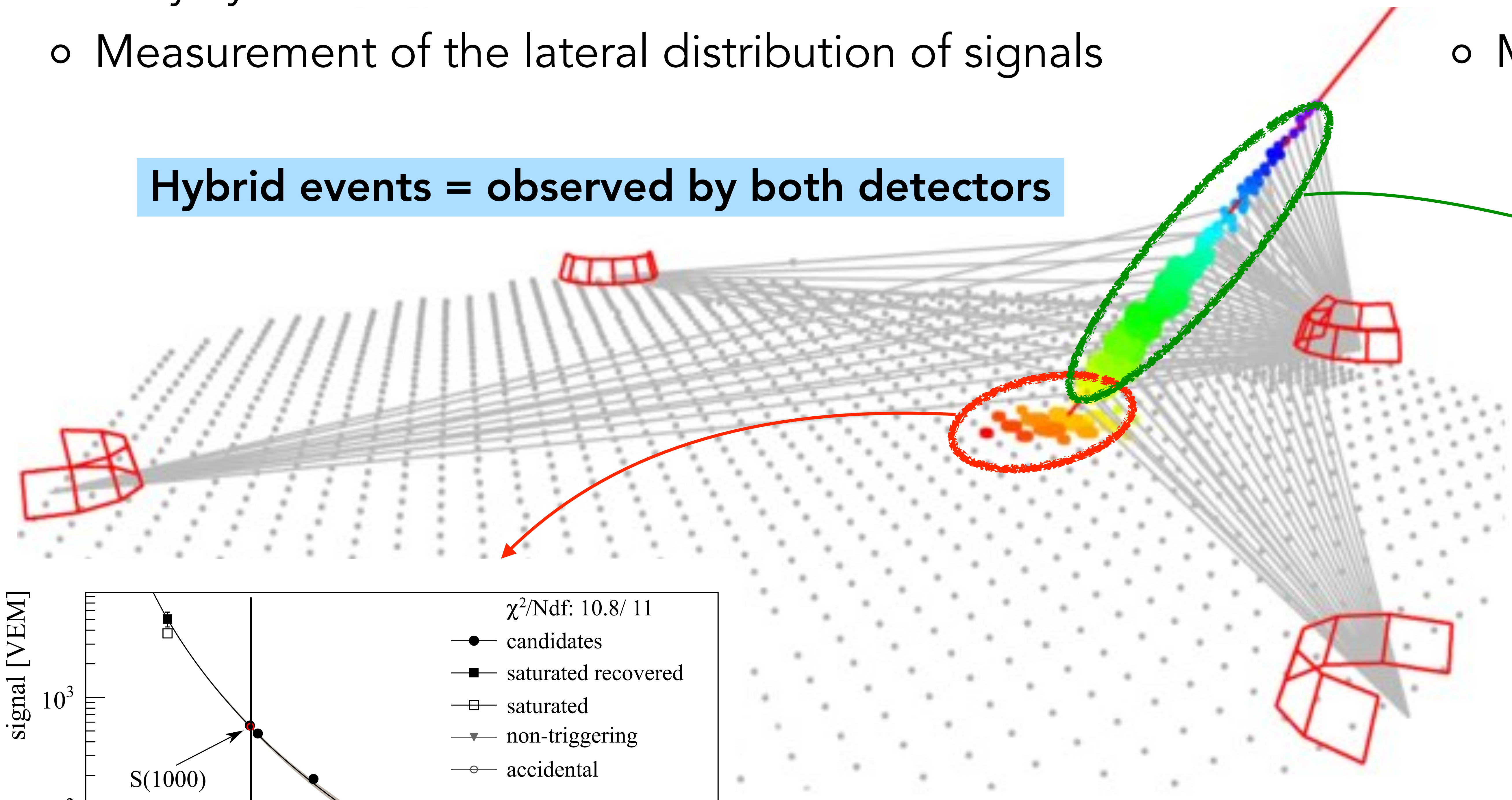

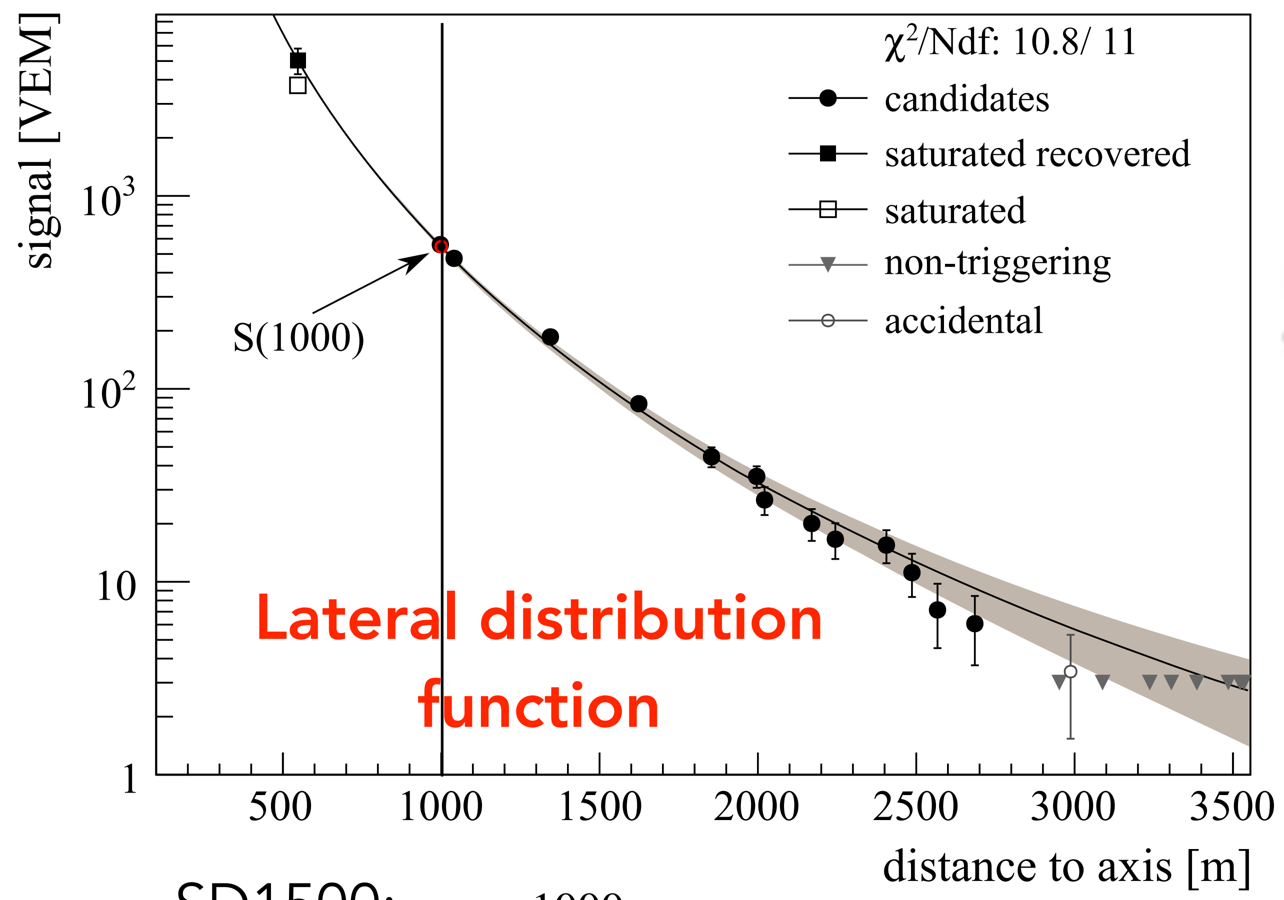

SD1500: $r_{opt} = 1000$ m

SD750 (Infill): $r_{opt} = 450$ m

Estimator S(r_{opt}) = shower size at a distance r_{opt} from the core

$$S(r) \propto r^{\beta}(r + r_M)^{\beta+\gamma} \rightarrow S(r_{opt})$$

Fluorescence Detector (FD)

- Duty cycle: ~15%
- Measurement of the longitudinal profile

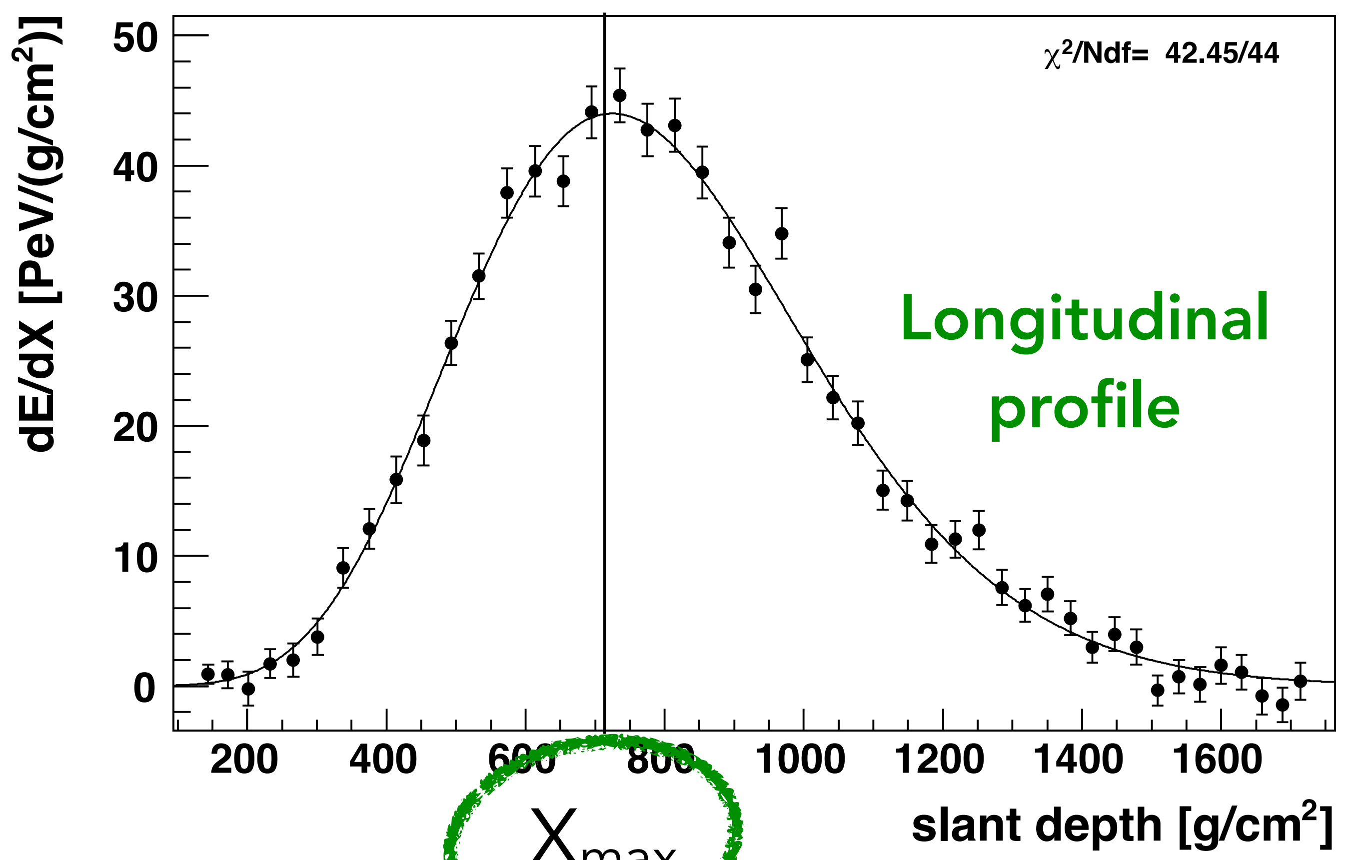

X_{max}

Depth of shower maximum

$$E_{cal} = \int \frac{dE}{dX} dX$$

Calorimetric energy

- X_{max} used as a **mass composition estimator for the FD events**
- **Energy of all the SD events** obtained through the calibration between S and E_{cal} with the hybrid events

Energy spectrum and mass composition measurements

Energy spectrum for the events measured with the SD array

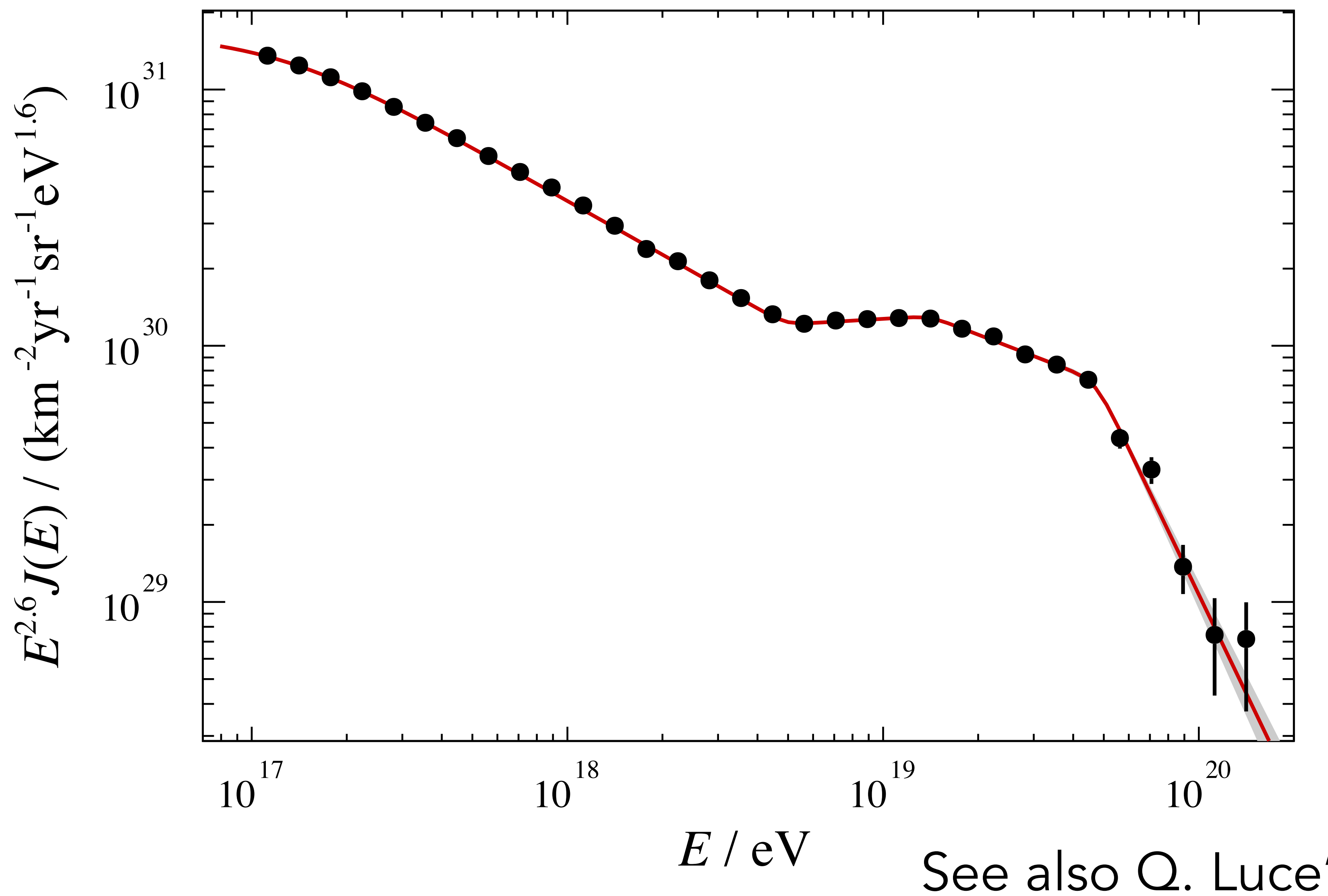

See also Q. Luce's talk at this conference

The X_{max} distribution in each energy bin is sensitive to the mass composition

→ **first two moments shown for figurative purposes**

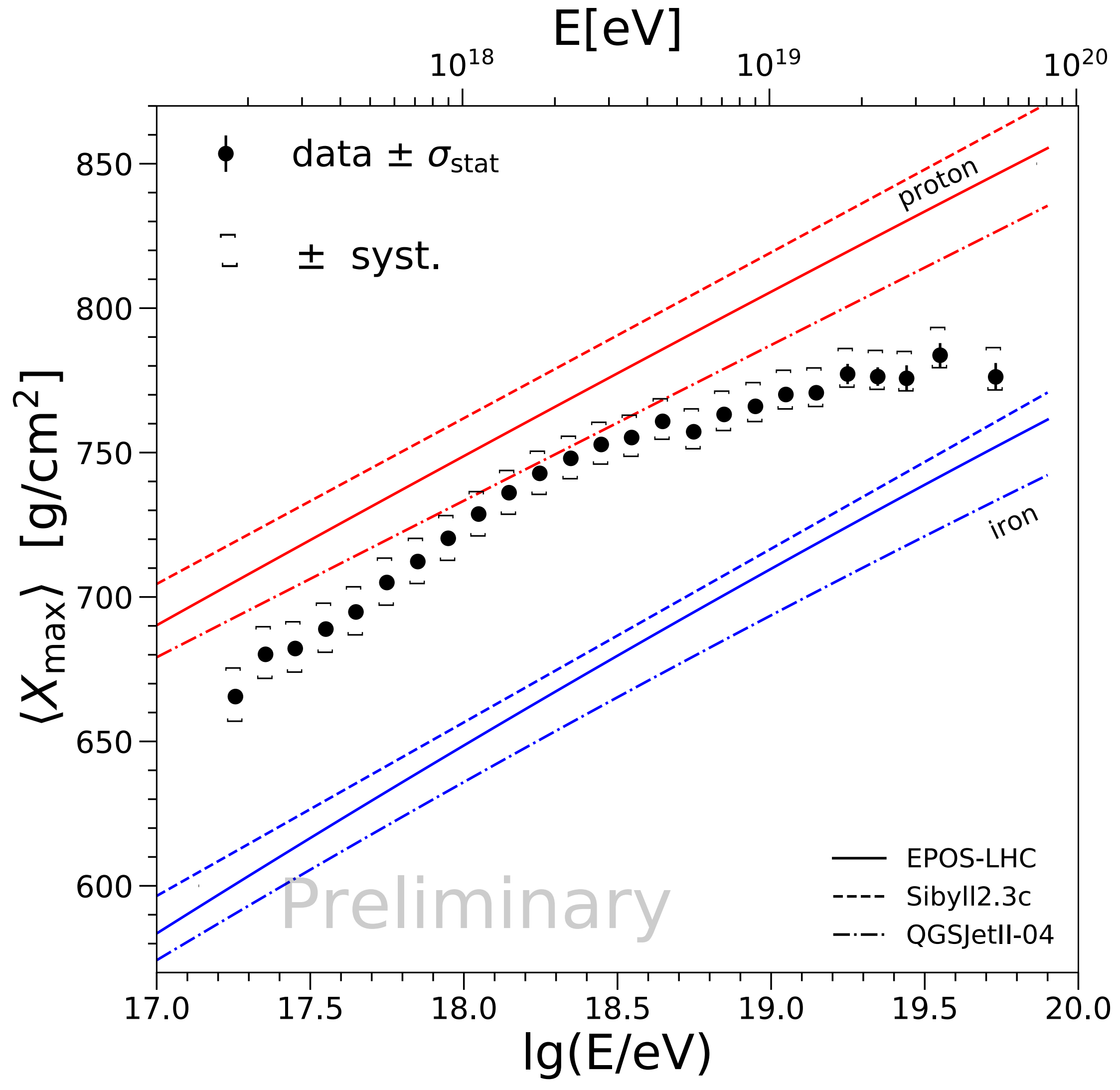

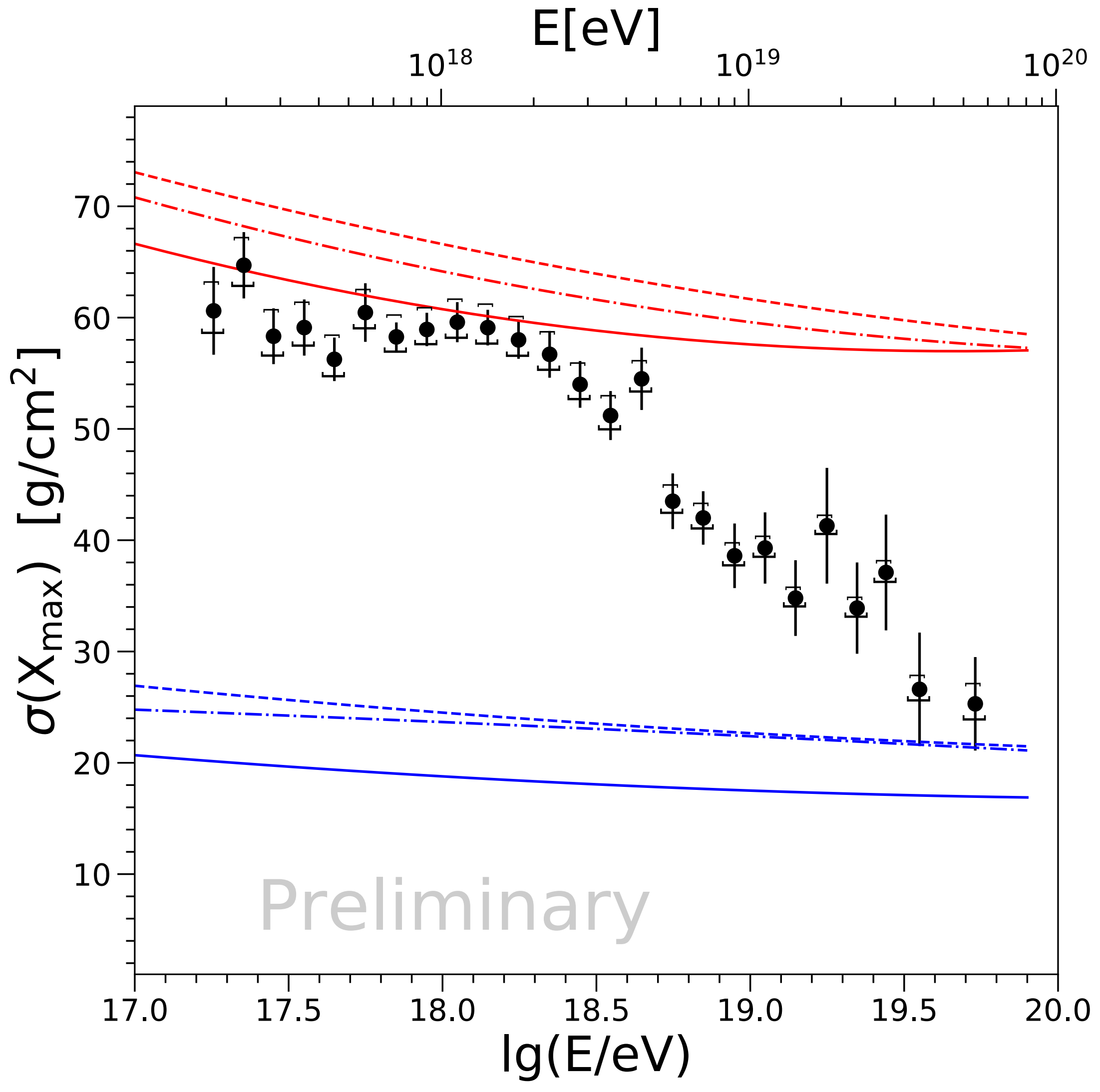

Data in $\log_{10}$(E/eV) bins of 0.1 width:

- Energy spectrum up to $10^{20.2}$ eV
- X_{max} distributions: up to $10^{19.7}$ eV (+ 1 additional bin for events above), binned in intervals of X_{max} of 20 g cm^{-2}

The Pierre Auger Collaboration, Eur. Phys. J. C 81, 966 (2021)
A.Yushkov for the Pierre Auger Collaboration PoS(ICRC2019)482

Energy spectrum and mass composition measurements

Energy spectrum for the events measured with the SD array

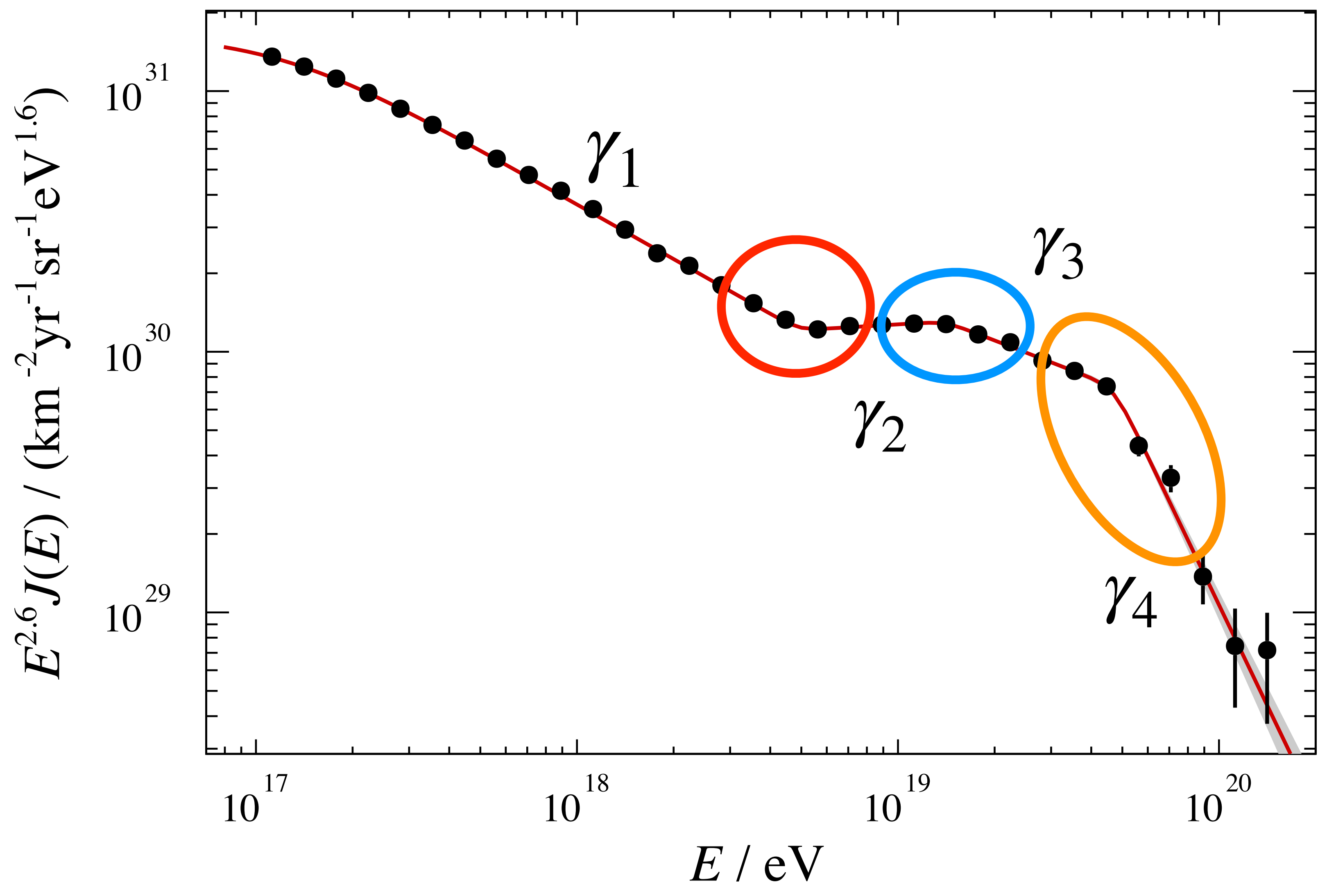

The X_{max} distribution in each energy bin is sensitive to the mass composition

→ **first two moments shown for figurative purposes**

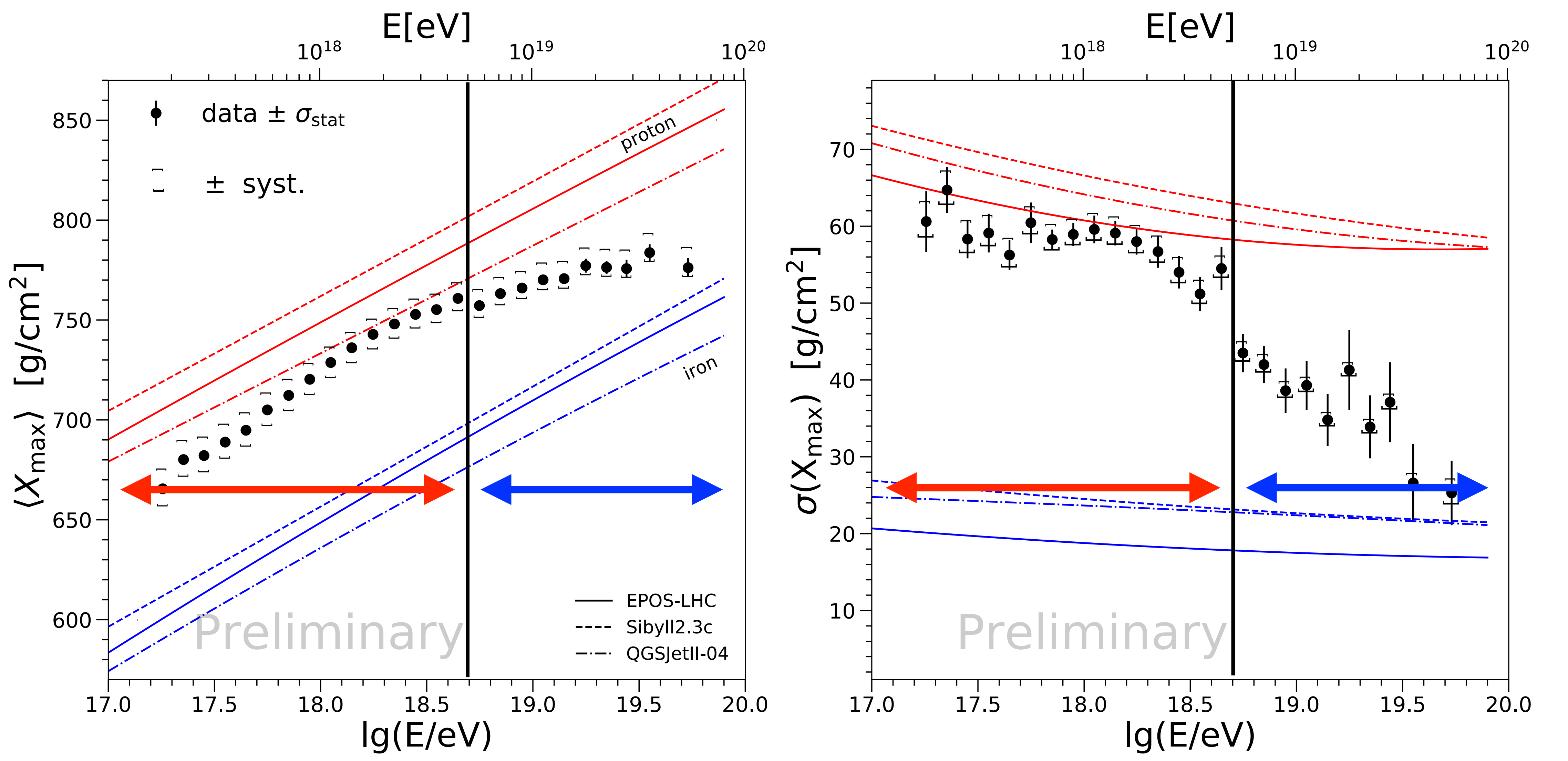

- **Hardening at ~6×10^{18} eV (ankle)**
- **Recently observed softening at ~1×10^{19} eV (instep)**
- **Suppression at ~5×10^{19} eV** → energy cut off

Propagation effect and/or maximum energy at the acceleration

- **Below the ankle: mass composition gets increasingly lighter**
- **At the ankle: mixed composition**
- **Above the ankle: increasingly heavier and less mixed**

→ superposition of alternating and heavier groups of elements

→ increasingly sparse statistics up to ~$10^{19.7}$ eV

The Pierre Auger Collaboration, Eur. Phys. J. C 81, 966 (2021)
A.Yushkov for the Pierre Auger Collaboration PoS(ICRC2019)482

Measurements of the energy spectrum and mass composition

Energy spectrum for the events measured with the SD array

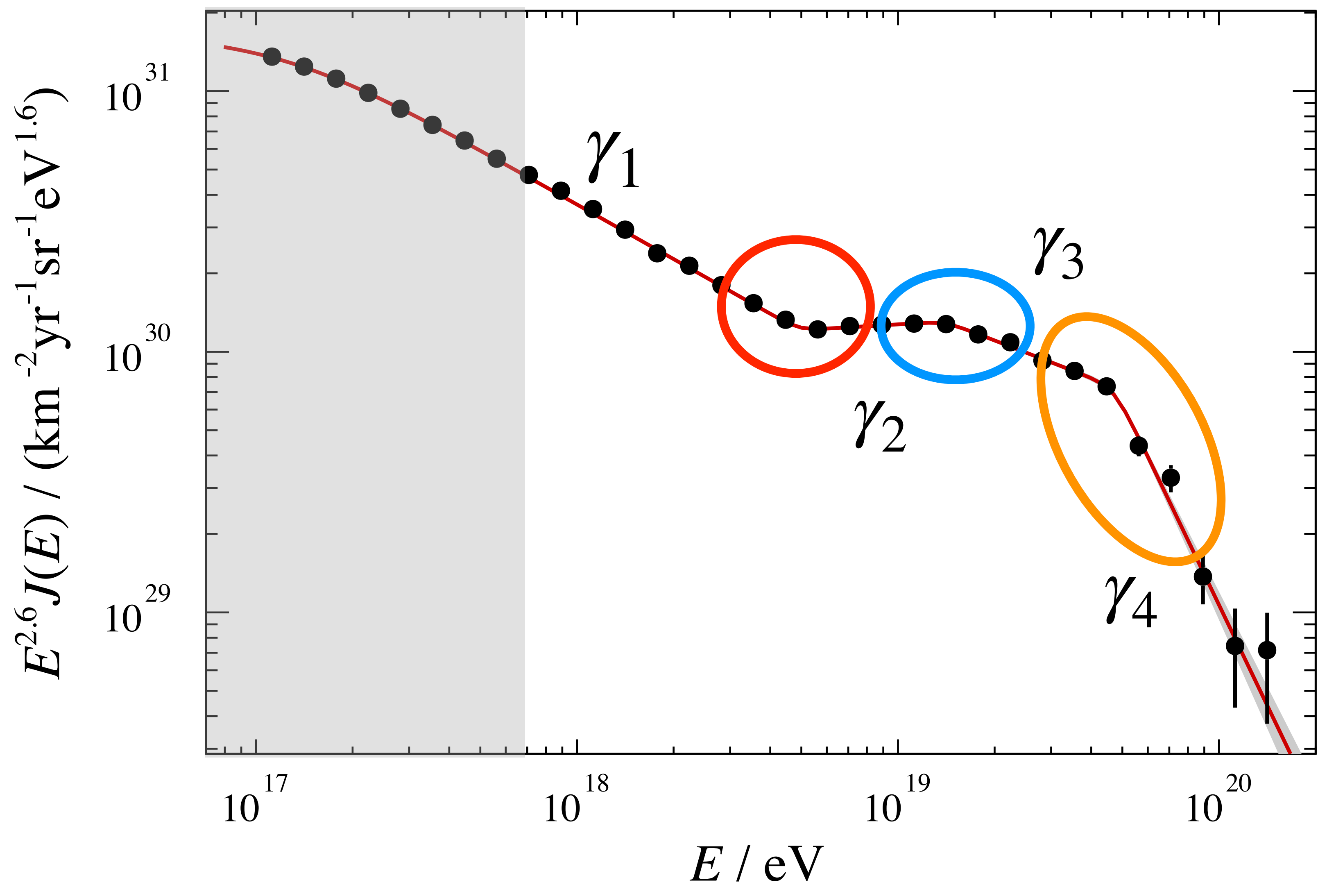

The X_{max} distribution in each energy bin is sensitive to the mass composition

→ **first two moments shown for figurative purposes**

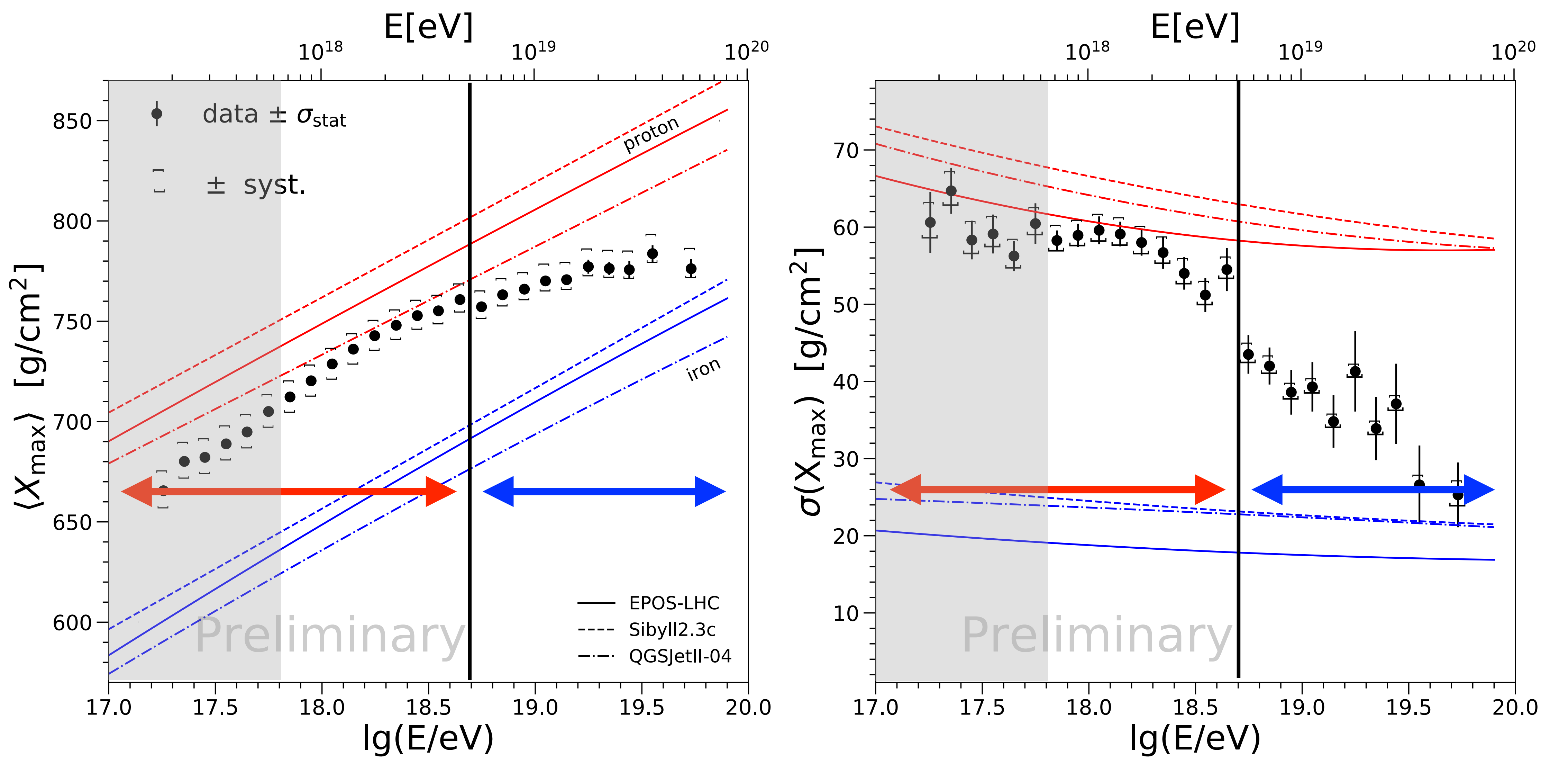

Combining the information from the two data sets is crucial to interpret the features

- We aim at including the ankle region
- We want to focus on the energy region the Galactic CRs are not dominant anymore

} **Data above E ~ 6 x 10^{17} eV are considered**

The Pierre Auger Collaboration, Eur. Phys. J. C 81, 966 (2021)
A.Yushkov for the Pierre Auger Collaboration PoS(ICRC2019)482

The combined fit

CRs ejected by EG accelerators

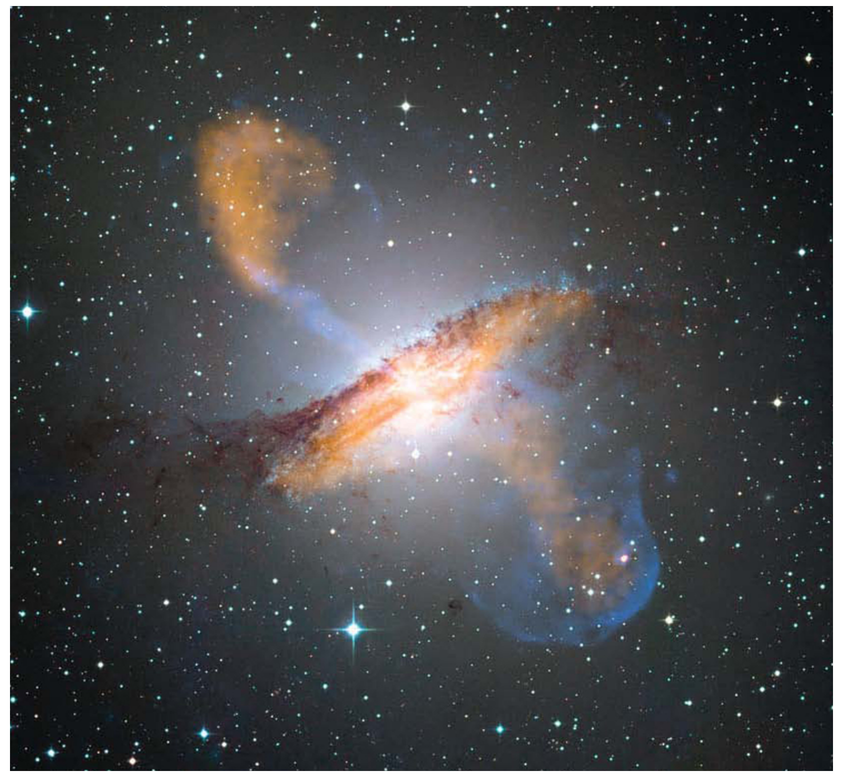

Assumptions on a simple astrophysical model

(CRs considered **at the escape**)

Propagation through the intergalactic medium +

SimProp[1] simulations

Choice of propagation models for uncertain quantities

Production of showers in the atmosphere

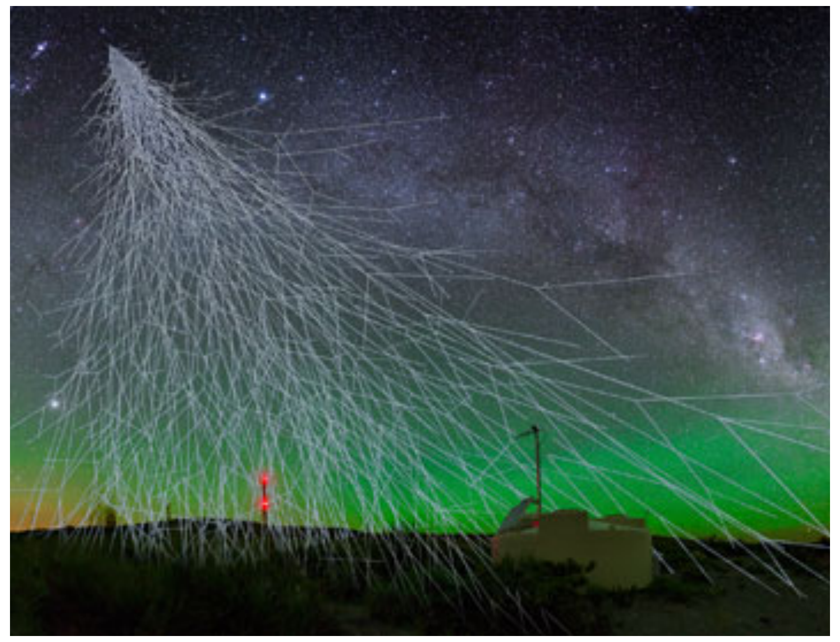

Choice of hadronic interaction models

Comparison with the data (detector effects are included)

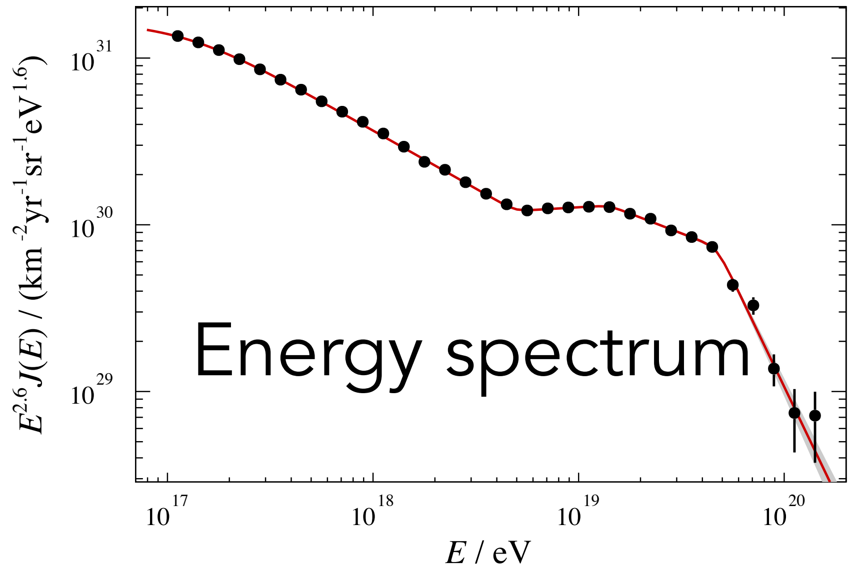

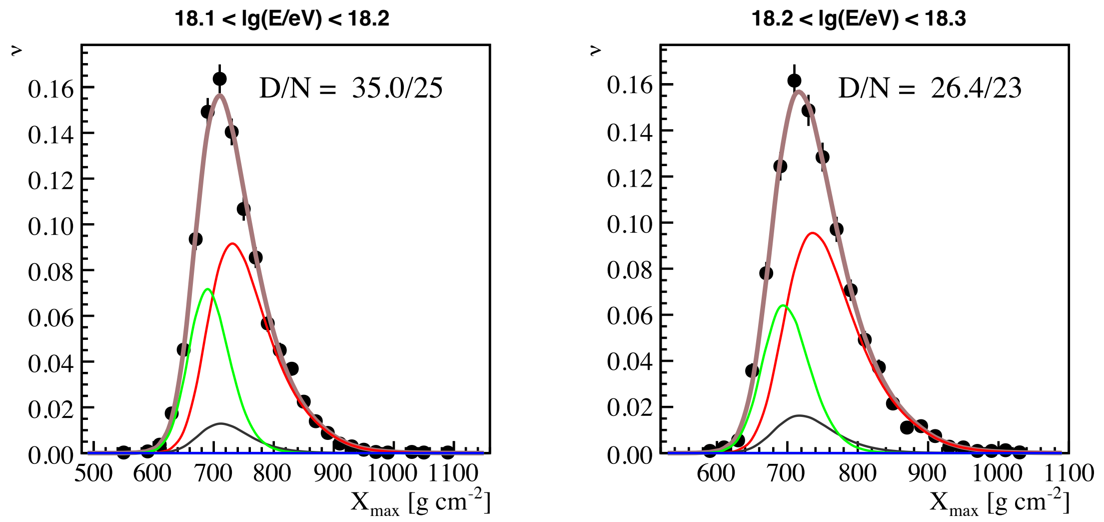

X_{max} distributions

Estimation of free parameters

→ characterization of the fluxes at the sources (energy spectrum & mass composition)

[1] R. Aloisio et al, JCAP 11 (2017) 009

Astrophysical model

Generic population of extragalactic sources

- population of identical sources
- uniform distribution (except for a local overdensity for $d < 30\ \mathrm{Mpc}$)
- ejection of **n representative nuclear species A**, chosen among ^{1}H, ^{4}He, ^{14}N, ^{28}Si, ^{56}Fe

Generation rate at the sources for each mass A (number of nuclei ejected per unit of energy, volume and time) **:**

$$\widetilde{Q}_A(E) = \widetilde{Q}_{0A} \cdot \left(\frac{E}{E_0}\right)^{-\gamma} \cdot \begin{cases} 1, & E \leq Z_A \cdot R_{\mathrm{cut}}; \\ \exp\left(1 - \frac{E}{Z_A \cdot R_{\mathrm{cut}}}\right), & E > Z_A \cdot R_{\mathrm{cut}}, \end{cases}$$

Characterizing the fluxes escaping the source environment → parameters estimated in the fit

- Spectral parameters γ, R_{cut}
- n partial normalisations $\widetilde{Q}_{0A}$

$$\widetilde{Q}_{0A} \longrightarrow I_A = \frac{\int_{E_{\min}}^{\infty} E \cdot \widetilde{Q}_A(E)\, dE}{\mathscr{L}_0}$$

Fractions of the total emissivity of sources above E_{min}= $10^{17.8}$ eV

$$with\ \ \mathscr{L}_0 = \sum_A \int_{E_{\min}}^{\infty} E \cdot \widetilde{Q}_A(E)\, dE$$

expressed in $\mathrm{erg} \cdot \mathrm{Mpc}^{-3} \cdot \mathrm{yr}^{-1}$

Emissivity of a population: total energy ejected per unit of comoving volume and time

Propagation model

Propagation through the IGM and the Earth's atmosphere

- **SimProp simulations** for the **propagation in the IGM** → **model for the photo-disintegration cross sections $\sigma_{\rm pd}$**
  → **model for the EBL spectrum and evolution**

  - Adiabatic energy losses (expansion of the Universe) $$-\left(\frac{1}{E}\frac{dE}{dt}\right)_{ad} = H_0\sqrt{(1+z)^3\Omega_m + \Omega_\Lambda}$$
  - Interactions of nuclei with background photons (EBL, CMB)
    - Photo-pion production $N + \gamma \rightarrow N + \pi^0 \ / \ N + \pi^{\pm}$
    - Pair production $N + \gamma \rightarrow N + e^+ + e^-$
    - Photo-disintegration $(A, Z) + \gamma \rightarrow (A - n, Z - n') + nN$

- **Hadronic interaction model** for the **propagation in the atmosphere**

- 1D propagation → intergalactic magnetic fields are here neglected

Model configuration used for our reference results:
Talys for $\sigma_{\rm pd}$, Gilmore model for EBL, EPOS-LHC as hadronic interaction model

J. Koning et al., vol. 769 of American Institute of Physics Conference Series, 2005
R. Gilmore et al., Mon. Not. Roy. Astron. Soc., 422 (2012) 3189
T. Pierog et al., Phys. Rev. C 92 (2015) 034906

Fit procedure

Combined fit of the energy spectrum and X_{max} distributions above $\sim 6 \times 10^{17}\mathrm{eV}$

→ compare simulated and measured fluxes at the Earth with the **maximum likelihood method**

$$D = D(J) + D(X_{\max}) = -2\ \ln\left(\frac{\mathscr{L}}{\mathscr{L}^{\mathrm{sat}}}\right) = -2\ \ln\left(\frac{\mathscr{L}_{\mathrm{J}}}{\mathscr{L}^{\mathrm{sat}}_{\mathrm{J}}}\right) - 2\ \ln\left(\frac{\mathscr{L}_{\mathrm{X_{max}}}}{\mathscr{L}^{\mathrm{sat}}_{\mathrm{X_{max}}}}\right)$$

- **Energy spectrum** → Gaussian distributions

$$L_{\mathrm{J}} = \prod_i \frac{1}{\sqrt{2\pi\sigma_i^2}} \exp\left(-\frac{(J_i^{\mathrm{obs}} - J_i^{\mathrm{mod}})^2}{2\sigma_i^2}\right),$$

observed unfolded flux
(detector effects)
expected simulated flux

- **X_{max} distributions** → multinomial distributions

$$L_{\mathrm{X_{max}}} = \sum_i n_i^{\mathrm{obs}}! \sum_j \frac{1}{k_{i,j}^{\mathrm{obs}}!} (G_{i,j}^{\mathrm{mod}})^{k_{i,j}^{\mathrm{obs}}}$$

observed events
model probability
(Gumbel distribution + detector effects)

i = $\log_{10}$(E) bin, j = X_{max} bin

$$D = D(J) + D(X_{\max}) = \sum_i \frac{(J_i^{\mathrm{obs}} - J_i^{\mathrm{mod}})^2}{\sigma_i^2} + 2 \cdot \sum_i \sum_{k_{i,j}^{\mathrm{obs}}} k_{i,j}^{\mathrm{obs}} \cdot \ln\left(\frac{k_{i,j}^{\mathrm{obs}}}{n_i^{\mathrm{obs}} \cdot G_{i,j}^{\mathrm{mod}}}\right)$$

→ The observed and simulated fluxes are compared by minimising the deviance D

The reference scenarios

✳ **Superposition of two (or more) populations to describe the ankle feature**

✳ The extragalactic components ejected according to a power law with a rigidity dependent cutoff (with different parameters)

SCENARIO 1 : EXTRAGALACTIC AND GALACTIC POPULATIONS

- **Extragalactic populations with mixed mass composition** dominating at high energy (HE)
- **Extragalactic population of pure protons** dominating at low energy (LE)
  → Possibly produced by decay of neutrons from photodisintegrations of nuclei in the same source environment
- **Galactic additional contribution** at low energy (considered at the Earth → no propagation included)
  → the best fit is given by a nitrogen component extending up to $Z \cdot R_{\mathrm{cut}}^{\mathrm{Gal}} \approx 2 \cdot 10^{18}$ eV

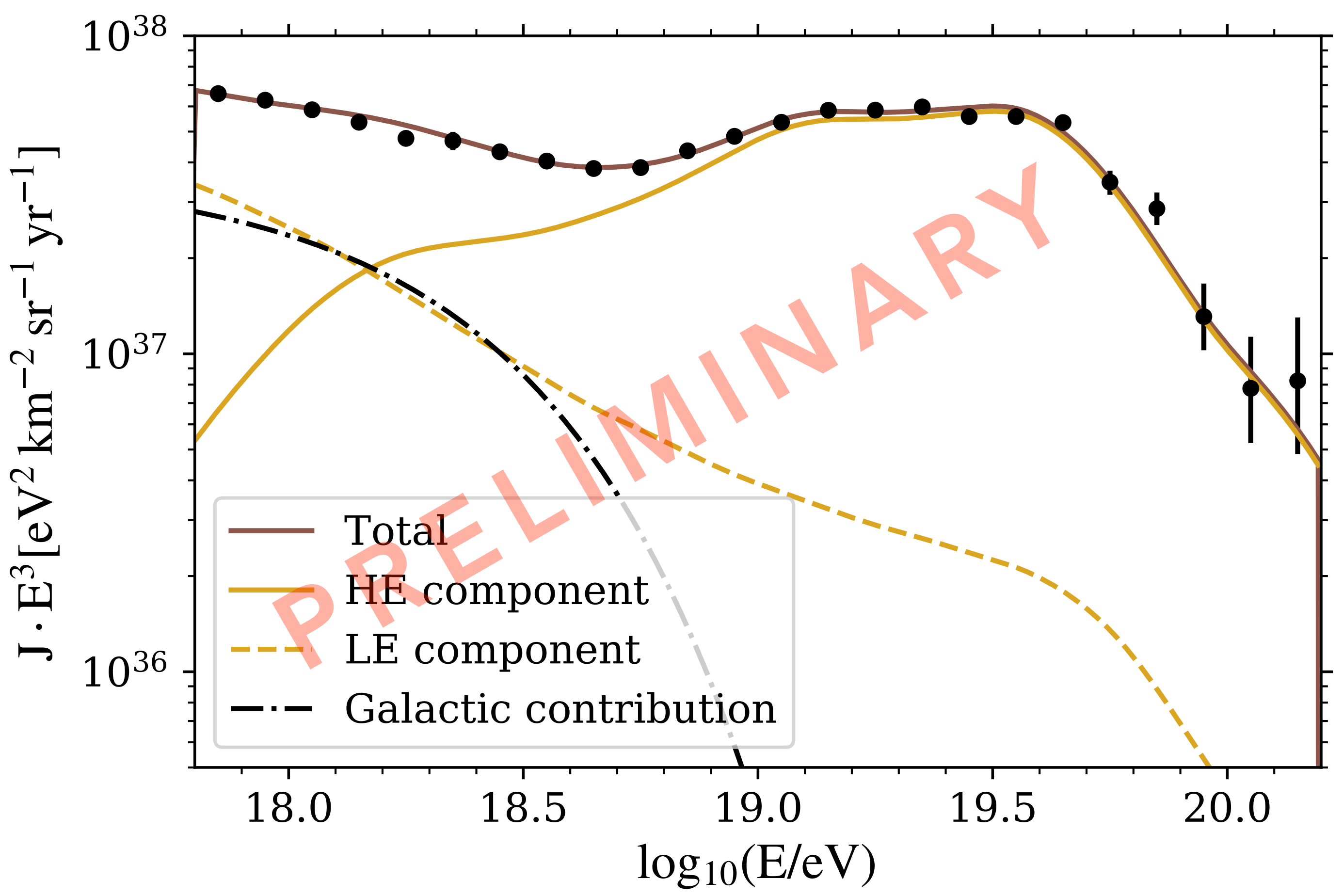

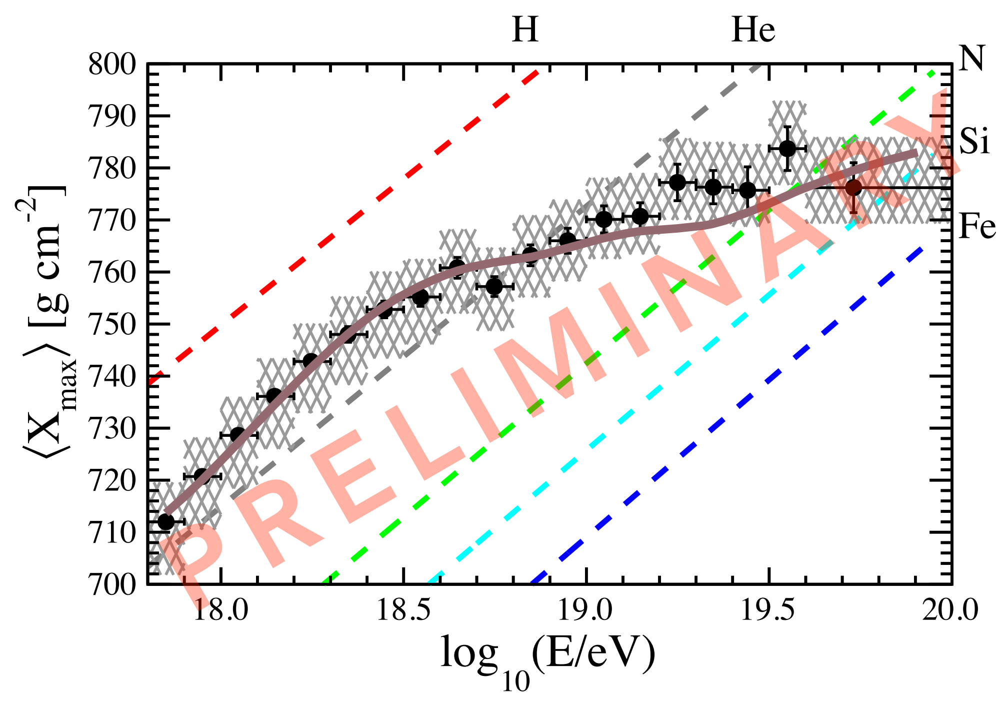

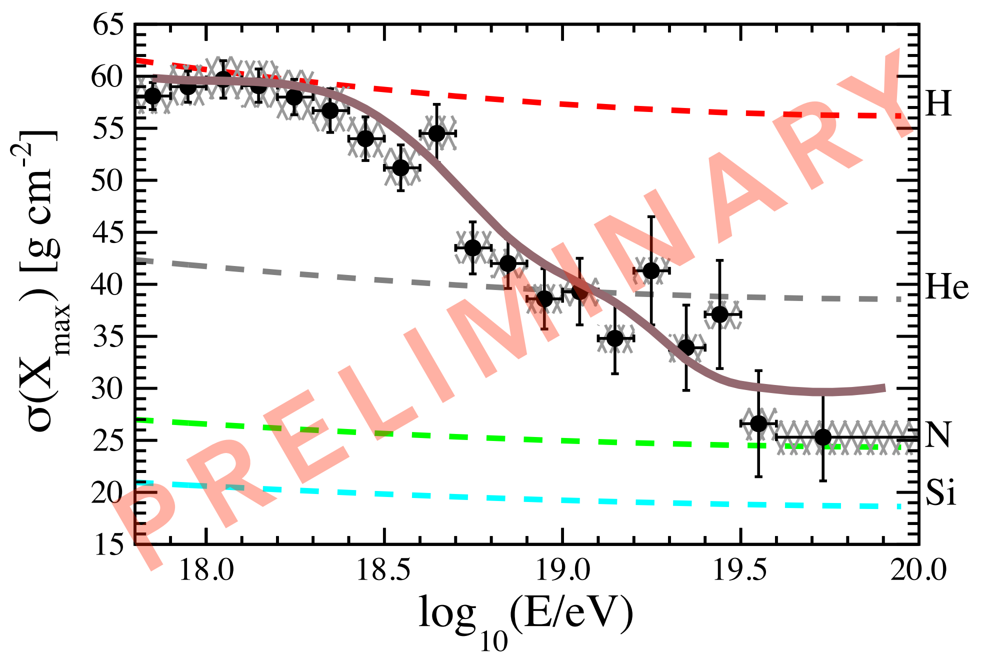

The reference scenarios

* ✳ **Superposition of two (or more) populations to describe the ankle feature**
* ✳ The extragalactic components ejected according to a power law with a rigidity dependent cutoff (with different parameters)

SCENARIO 2 : TWO MIXED EXTRAGALACTIC POPULATIONS

- **Extragalactic populations with mixed mass composition** dominating at high energy (HE)
- **Extragalactic population with mixed mass composition** dominating at low energy (LE)

→ produced by two different populations of sources

→ Galactic contributions are subdominant in this energy range

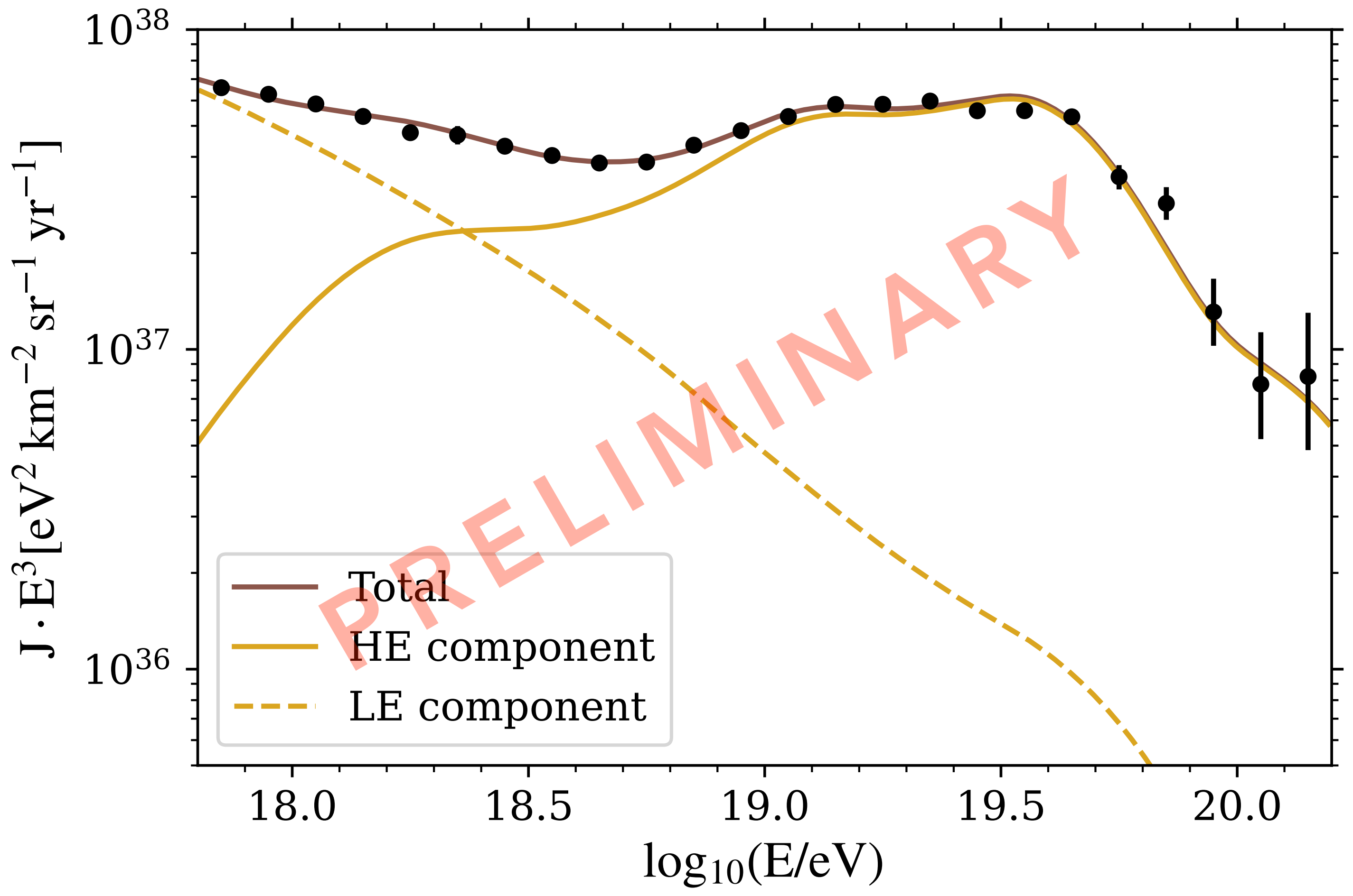

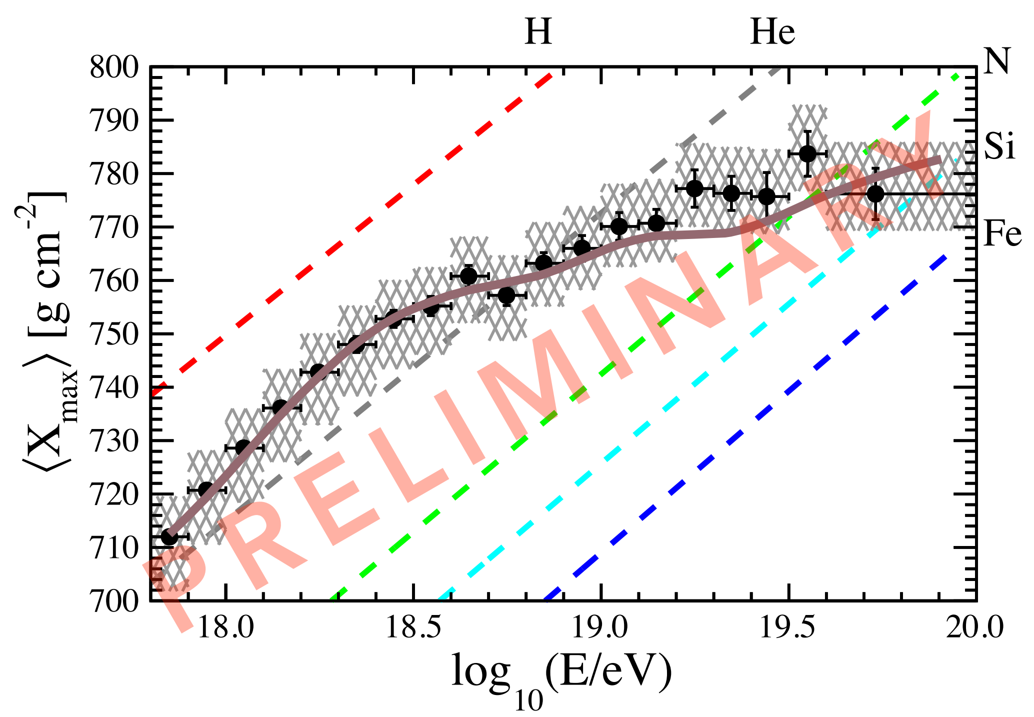

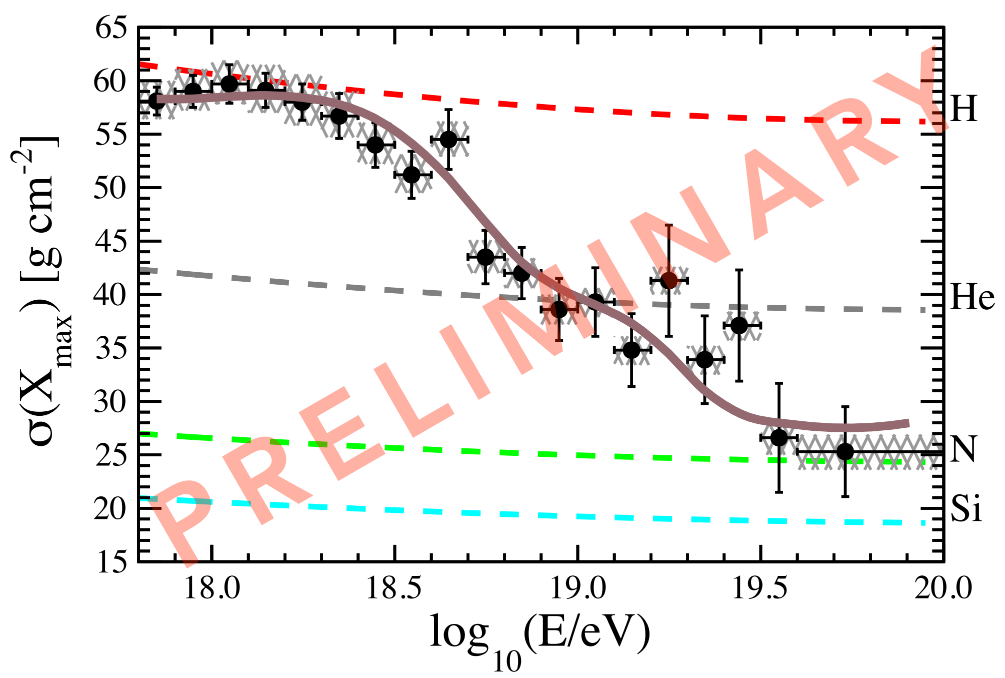

Results in the reference scenarios

	Scenario 1		Scenario 2	
Galactic contribution (at Earth)	pure N		—	
J_0^{Gal} $[\mathrm{eV}^{-1} \cdot \mathrm{km}^{-2} \cdot \mathrm{sr}^{-1} \cdot \mathrm{yr}^{-1}]$	$(1.06 \pm 0.04) \cdot 10^{-13}$		—	
$\log_{10}(R_{\mathrm{cut}}^{\mathrm{Gal}}/\mathrm{V})$	17.48 ± 0.02		—	
EG components (at the escape)	LE	HE	LE	HE
$\mathcal{L}_0$ $[10^{44} \cdot \mathrm{erg} \cdot \mathrm{Mpc}^{-3} \cdot \mathrm{yr}^{-1}]$ *	6.54 ± 0.36	5.00 ± 0.35	11.35 ± 0.15	5.07 ± 0.06
γ	3.34 ± 0.07	-1.47 ± 0.13	3.52 ± 0.03	-1.99 ± 0.11
$\log_{10}(R_{\mathrm{cut}}/\mathrm{V})$	> 19.3	18.19 ± 0.02	> 19.4	18.15 ± 0.01
I_{H} (%)	100 (fixed)	0.0 ± 0.0	48.7 ± 0.3	0.0 ± 0.0
I_{He} (%)	—	24.5 ± 3.0	7.3 ± 0.4	23.6 ± 1.6
I_{N} (%)	—	68.1 ± 5.0	44.0 ± 0.4	72.1 ± 3.3
I_{Si} (%)	—	4.9 ± 3.9	0.0 ± 0.0	1.3 ± 1.3
I_{Fe} (%)	—	2.5 ± 0.2	0.0 ± 0.0	3.1 ± 1.3
D_J (N_J)	48.6 (24)		56.6 (24)	
$D_{X_{\max}}$ $(N_{X_{\max}})$	537.4 (329)		516.5 (329)	
D (N)	586.0 (353)		573.1 (353)	

* from $E_{\min} = 10^{17.8}$ eV.

Results in the reference scenarios

Some common findings between the two scenarios:

Very hard energy spectrum for the HE extragalactic component

- little overlap between different masses
  → description of very pronounced spectral features and narrow X_{max} distributions.
- Considering only the extragalactic propagation
  → energy-dependent effects in the source environment are not included
- "Magnetic horizon" effect
  → observed harder spectrum because of the suppression of the low-energy fluxes

	Scenario 1		Scenario 2	
Galactic contribution (at Earth)	pure N		—	
J_0^{Gal} [$\mathrm{eV}^{-1}\cdot\mathrm{km}^{-2}\cdot\mathrm{sr}^{-1}\cdot\mathrm{yr}^{-1}$]	$(1.06 \pm 0.04)\cdot 10^{-13}$		—	
$\log_{10}(R_{\mathrm{cut}}^{\mathrm{Gal}}/\mathrm{V})$	17.48 ± 0.02		—	
EG components (at the escape)	LE	HE	LE	HE
$\mathcal{L}_0$ [$10^{44}\cdot\mathrm{erg}\cdot\mathrm{Mpc}^{-3}\cdot\mathrm{yr}^{-1}$] *	6.54 ± 0.36	5.00 ± 0.35	11.35 ± 0.15	5.07 ± 0.06
γ	3.34 ± 0.07	-1.47 ± 0.13	3.52 ± 0.03	-1.99 ± 0.11
$\log_{10}(R_{\mathrm{cut}}/\mathrm{V})$	> 19.3	18.19 ± 0.02	> 19.4	18.15 ± 0.01
I_{H} (%)	100 (fixed)	0.0 ± 0.0	48.7 ± 0.3	0.0 ± 0.0
I_{He} (%)	—	24.5 ± 3.0	7.3 ± 0.4	23.6 ± 1.6
I_{N} (%)	—	68.1 ± 5.0	44.0 ± 0.4	72.1 ± 3.3
I_{Si} (%)	—	4.9 ± 3.9	0.0 ± 0.0	1.3 ± 1.3
I_{Fe} (%)	—	2.5 ± 0.2	0.0 ± 0.0	3.1 ± 1.3
D_J (N_J)	48.6 (24)		56.6 (24)	
$D_{X_{\max}}$ ($N_{X_{\max}}$)	537.4 (329)		516.5 (329)	
D (N)	586.0 (353)		573.1 (353)	

* from $E_{\min} = 10^{17.8}$ eV.

PRELIMINARY

Generation rate at the sources

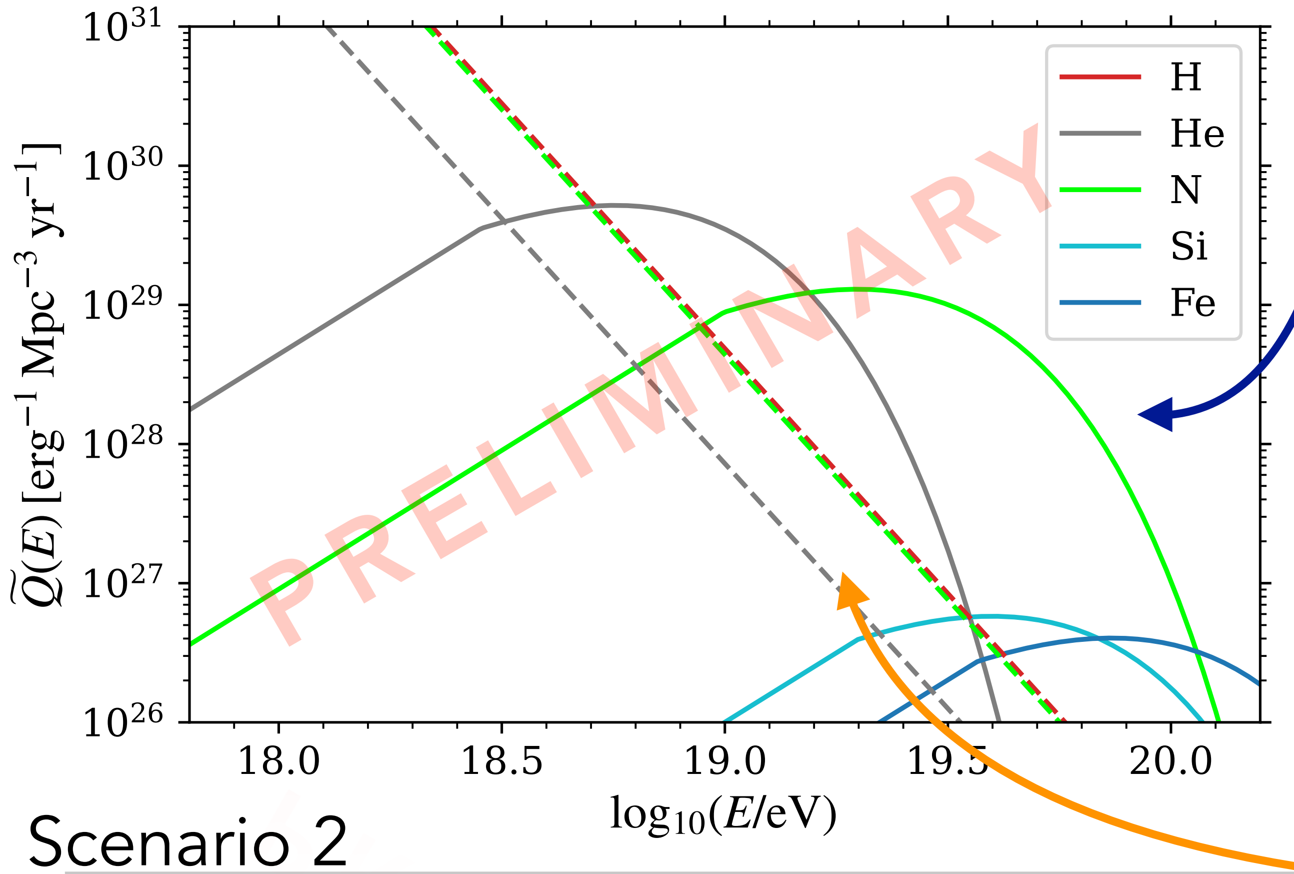

Scenario 2

Energy spectrum at the Earth

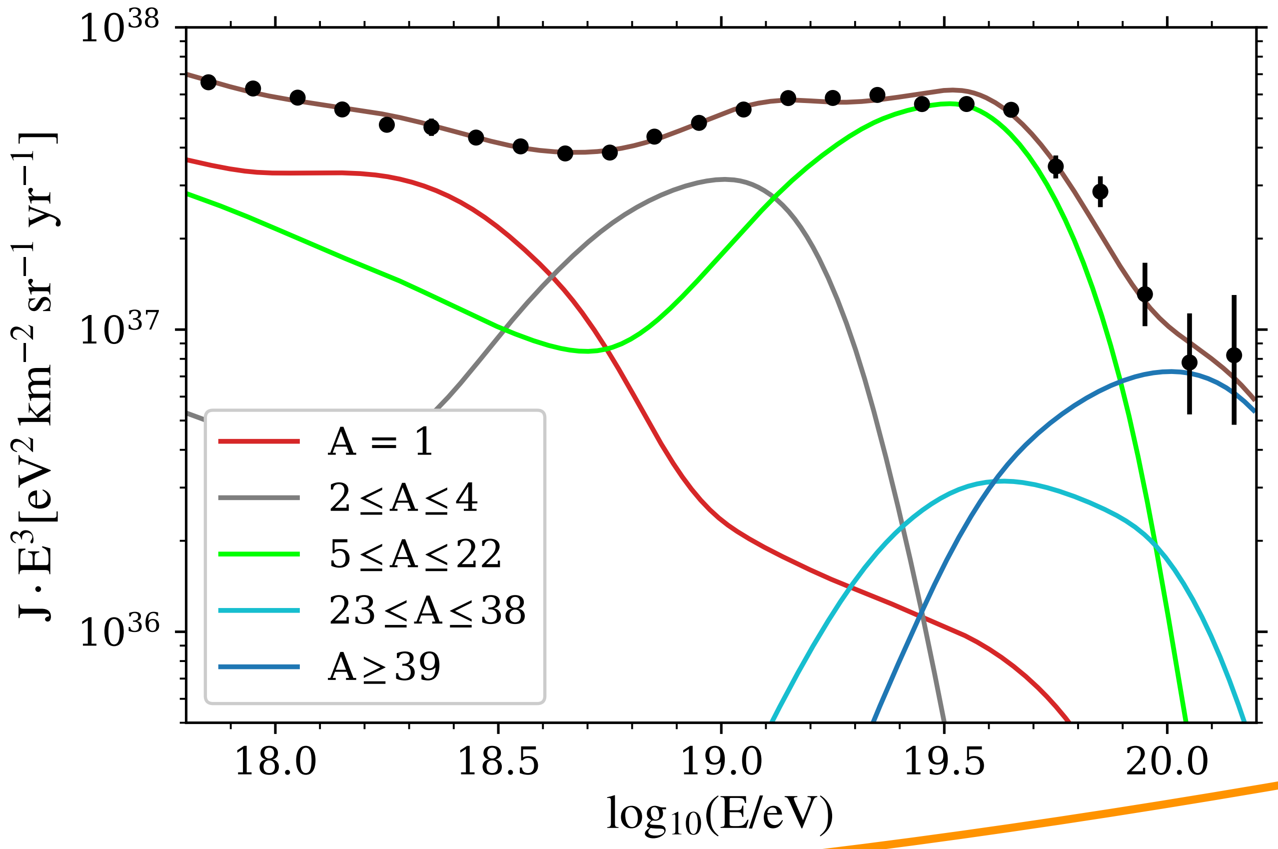

Very soft energy spectrum for the LE extragalactic component

Possible explanation:

- Sources with different maximal energies (not identical)
  → the energy spectrum of each source may be less steep

Results in the reference scenarios

Some common findings between the two scenarios:

Low rigidity cutoff of the HE component

- It affects the observed fluxes ($< 10^{18.5}$ eV)
  → <u>but</u> not low enough to make propagation effects negligible

Mixed mass composition of the HE component

- No mass composition information at the highest energies
  → fit based on the shape of the energy spectrum

	Scenario 1		Scenario 2	
Galactic contribution (at Earth)	pure N		—	
J_0^{Gal} $[\mathrm{eV^{-1} \cdot km^{-2} \cdot sr^{-1} \cdot yr^{-1}}]$	$(1.06 \pm 0.04) \cdot 10^{-13}$		—	
$\log_{10}(R_{\mathrm{cut}}^{\mathrm{Gal}}/\mathrm{V})$	17.48 ± 0.02		—	
EG components (at the escape)	LE	HE	LE	HE
$\mathcal{L}_0$ $[10^{44} \cdot \mathrm{erg \cdot Mpc^{-3} \cdot yr^{-1}}]$ *	6.54 ± 0.36	5.00 ± 0.35	11.35 ± 0.15	5.07 ± 0.06
γ	3.34 ± 0.07	-1.47 ± 0.13	3.52 ± 0.03	-1.99 ± 0.11
$\log_{10}(R_{\mathrm{cut}}/\mathrm{V})$	> 19.3	18.19 ± 0.02	> 19.4	18.15 ± 0.01
I_{H} (%)	100 (fixed)	0.0 ± 0.0	48.7 ± 0.3	0.0 ± 0.0
I_{He} (%)	—	24.5 ± 3.0	7.3 ± 0.4	23.6 ± 1.6
I_{N} (%)	—	68.1 ± 5.0	44.0 ± 0.4	72.1 ± 3.3
I_{Si} (%)	—	4.9 ± 3.9	0.0 ± 0.0	1.3 ± 1.3
I_{Fe} (%)	—	2.5 ± 0.2	0.0 ± 0.0	3.1 ± 1.3
D_J (N_J)	48.6 (24)		56.6 (24)	
$D_{X_{\max}}$ $(N_{X_{\max}})$	537.4 (329)		516.5 (329)	
D (N)	586.0 (353)		573.1 (353)	

* from $E_{\min} = 10^{17.8}$ eV.

PRELIMINARY

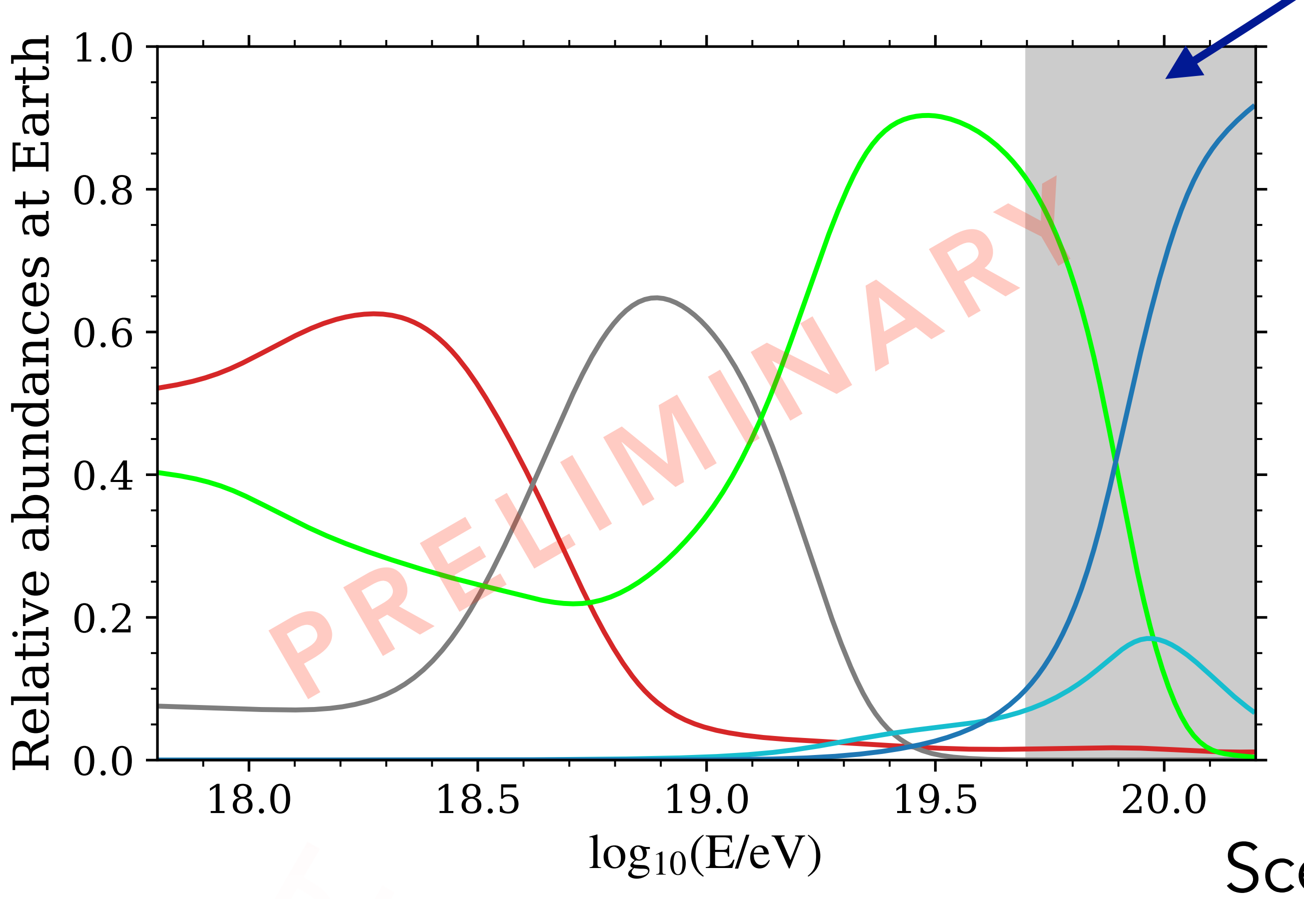

Scenario 2

Energy spectrum at the Earth

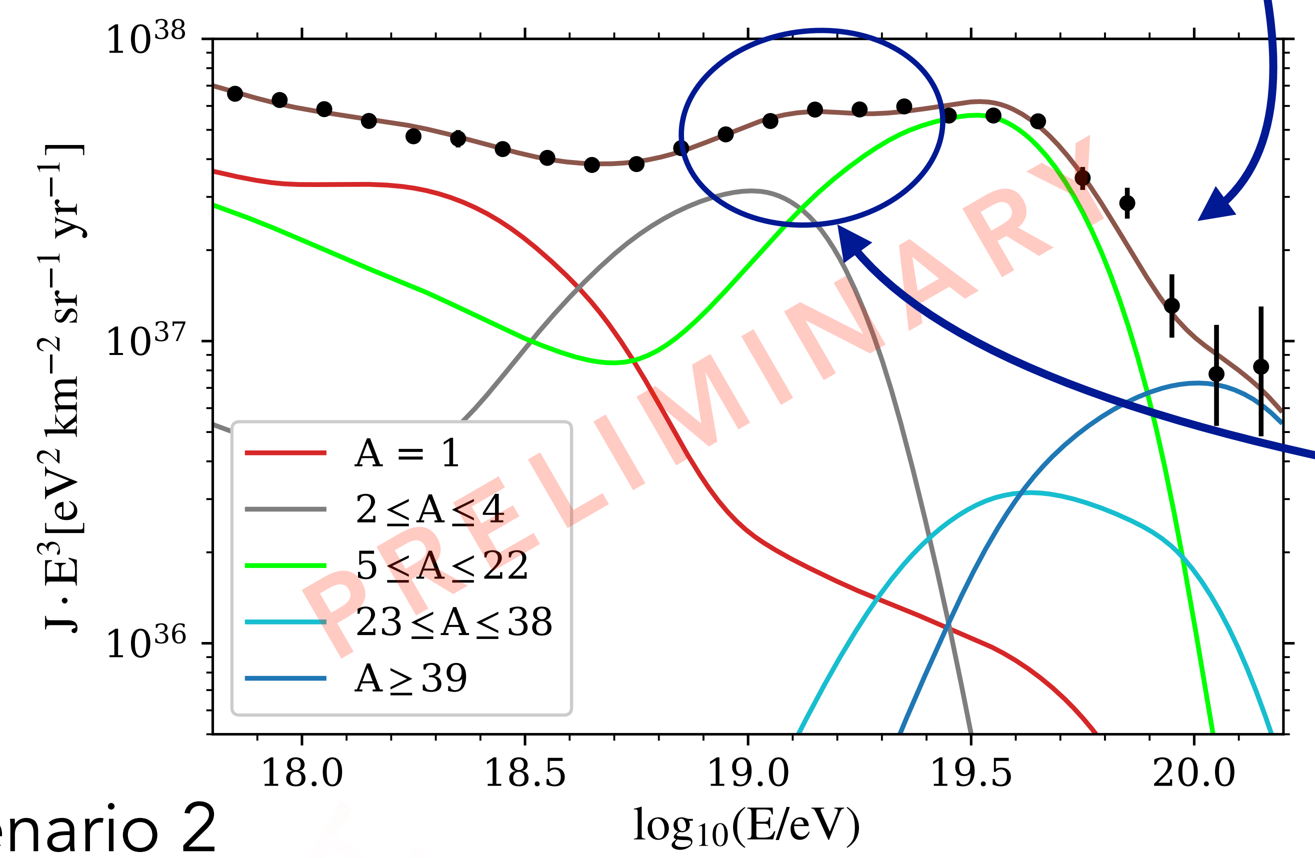

New observed feature at 13 EeV

→ interplay between He and N components ejected at the sources according to their R-dependent cutoff and then shaped by propagation

Results in the reference scenarios

Some common findings between the two scenarios:

Very high rigidity cutoff of the LE component

- Degenerate fit for $R_{cut}^{LE} \gg 10^{19.5}\mathrm{eV}$
  - → fixing the parameter to any much higher value does not change the fit
  - → only the lower bound
- The LE component is very steep
  - → dominant only in the first energy bins
  - → not very sensitive to the energy spectrum shape

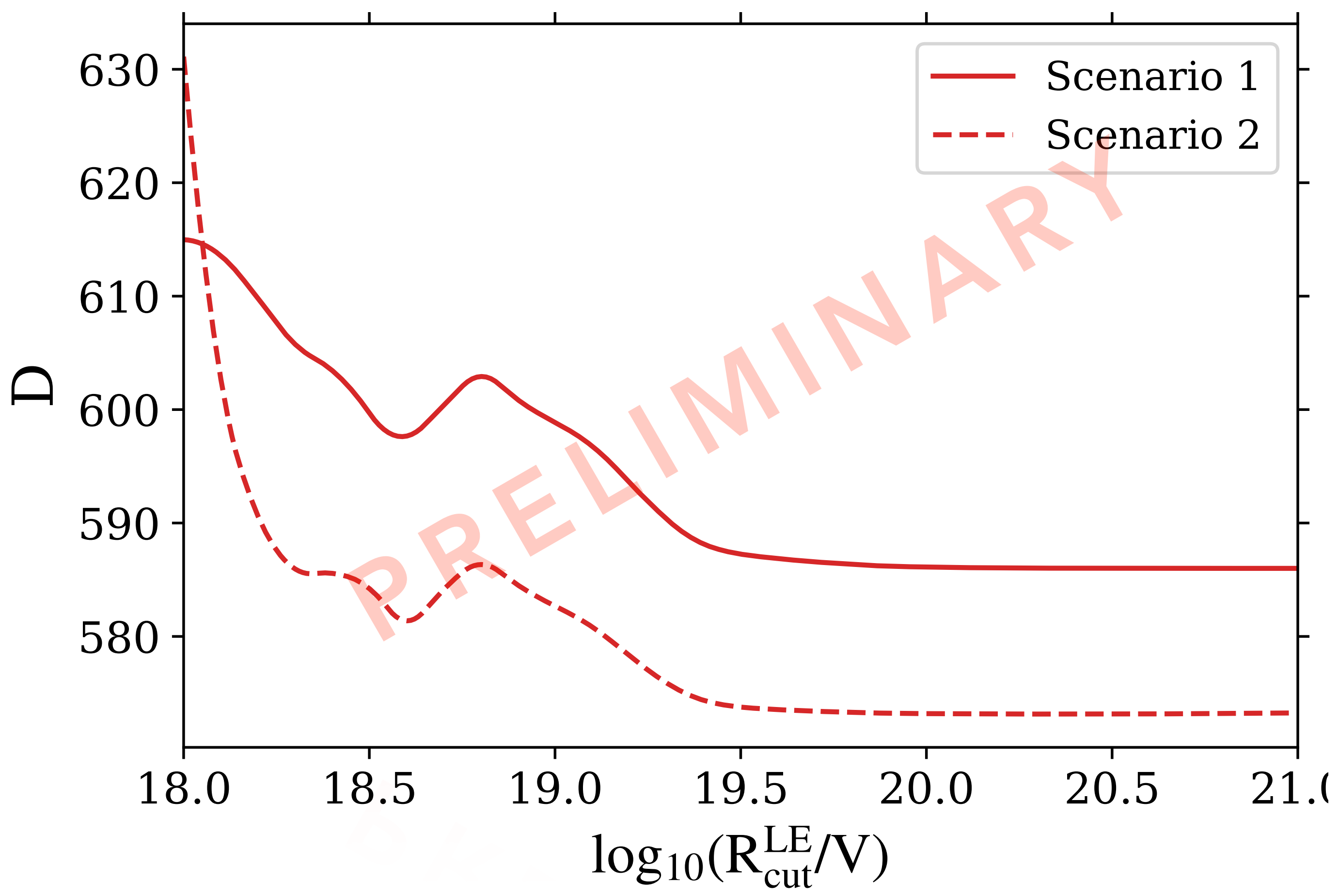

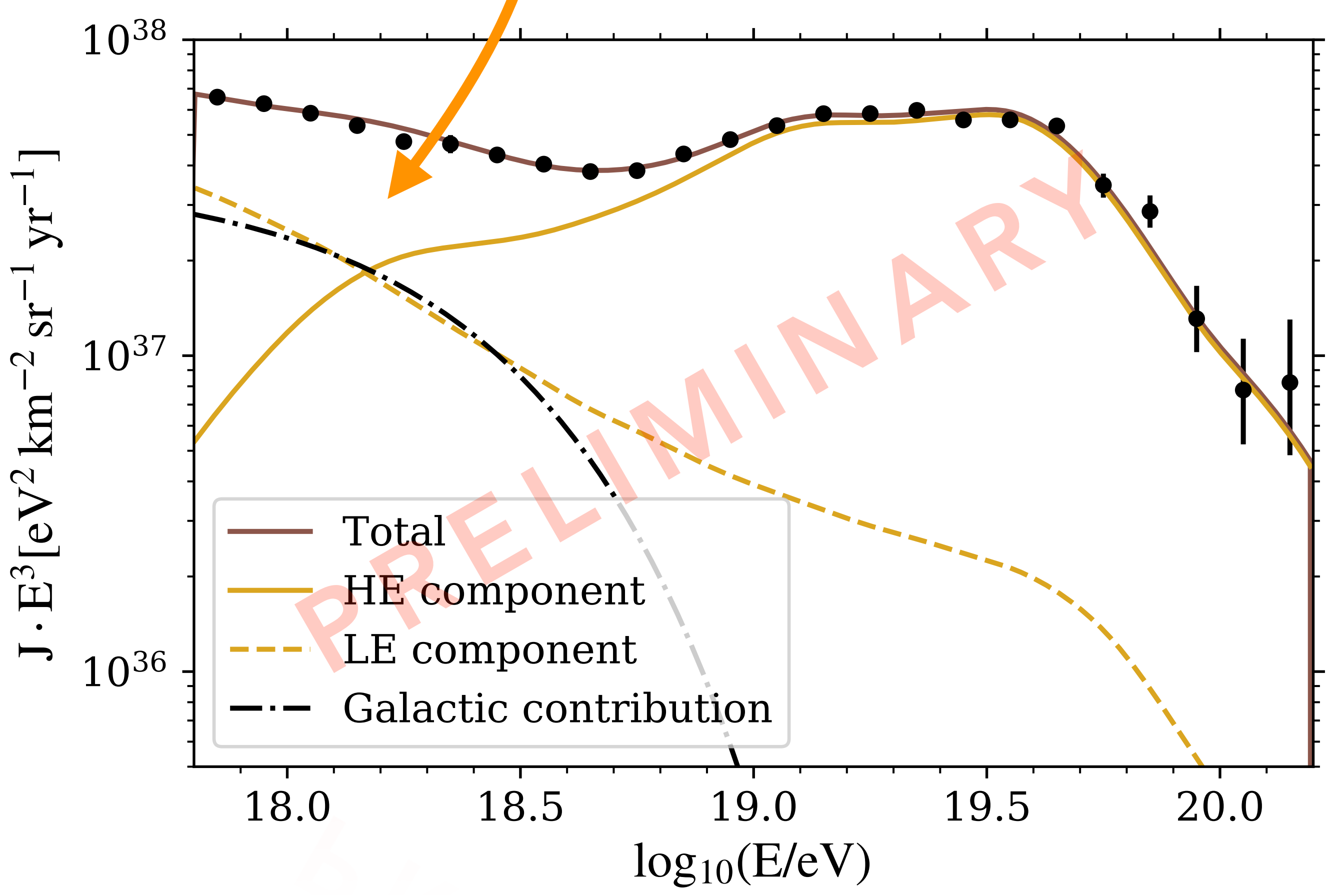

	SCENARIO 1		SCENARIO 2	
Galactic contribution (at Earth)	pure N		—	
J_0^{Gal} $[\mathrm{eV}^{-1} \cdot \mathrm{km}^{-2} \cdot \mathrm{sr}^{-1} \cdot \mathrm{yr}^{-1}]$	$(1.06 \pm 0.04) \cdot 10^{-13}$		—	
$\log_{10}(R_{\mathrm{cut}}^{\mathrm{Gal}}/\mathrm{V})$	17.48 ± 0.02		—	
EG components (at the escape)	LE	HE	LE	HE
$\mathcal{L}_0$ $[10^{44} \cdot \mathrm{erg} \cdot \mathrm{Mpc}^{-3} \cdot \mathrm{yr}^{-1}]$ *	6.54 ± 0.36	5.00 ± 0.35	11.35 ± 0.15	5.07 ± 0.06
γ	3.34 ± 0.07	-1.47 ± 0.13	3.52 ± 0.03	-1.99 ± 0.11
$\log_{10}(R_{\mathrm{cut}}/\mathrm{V})$	> 19.3	18.19 ± 0.02	> 19.4	18.15 ± 0.01
I_{H} (%)	100 (fixed)	0.0 ± 0.0	48.7 ± 0.3	0.0 ± 0.0
I_{He} (%)	—	24.5 ± 3.0	7.3 ± 0.4	23.6 ± 1.6
I_{N} (%)	—	68.1 ± 5.0	44.0 ± 0.4	72.1 ± 3.3
I_{Si} (%)	—	4.9 ± 3.9	0.0 ± 0.0	1.3 ± 1.3
I_{Fe} (%)	—	2.5 ± 0.2	0.0 ± 0.0	3.1 ± 1.3
D_J (N_J)	48.6 (24)		56.6 (24)	
$D_{X_{\max}}$ $(N_{X_{\max}})$	537.4 (329)		516.5 (329)	
D (N)	586.0 (353)		573.1 (353)	

* from $E_{\mathrm{min}} = 10^{17.8}$ eV.

PRELIMINARY

Results in the reference scenarios

The mass composition in the LE region

Mixture of H+N below the ankle in both scenarios

Galactic component in Scenario 1 :

- power law modified by an exponential cutoff with some free parameters
- Models with Galactic Fe/Si right below the ankle are strongly disfavored
- **a N-dominated composition is preferred**

  → contribution from explosions in the winds of Wolf-Rayet-like stars may provide N up to ~10^{18} eV

	Scenario 1		Scenario 2	
Galactic contribution (at Earth)	pure N		—	
J_0^{Gal} $[\mathrm{eV}^{-1} \cdot \mathrm{km}^{-2} \cdot \mathrm{sr}^{-1} \cdot \mathrm{yr}^{-1}]$	$(1.06 \pm 0.04) \cdot 10^{-13}$		—	
$\log_{10}(R_{\mathrm{cut}}^{\mathrm{Gal}}/\mathrm{V})$	17.48 ± 0.02		—	
EG components (at the escape)	LE	HE	LE	HE
$\mathcal{L}_0$ $[10^{44} \cdot \mathrm{erg} \cdot \mathrm{Mpc}^{-3} \cdot \mathrm{yr}^{-1}]$ *	6.54 ± 0.36	5.00 ± 0.35	11.35 ± 0.15	5.07 ± 0.06
γ	3.34 ± 0.07	-1.47 ± 0.13	3.52 ± 0.03	-1.99 ± 0.11
$\log_{10}(R_{\mathrm{cut}}/\mathrm{V})$	> 19.3	18.19 ± 0.02	> 19.4	18.15 ± 0.01
I_{H} (%)	100 (fixed)	0.0 ± 0.0	48.7 ± 0.3	0.0 ± 0.0
I_{He} (%)	—	24.5 ± 3.0	7.3 ± 0.4	23.6 ± 1.6
I_{N} (%)	—	68.1 ± 5.0	44.0 ± 0.4	72.1 ± 3.3
I_{Si} (%)	—	4.9 ± 3.9	0.0 ± 0.0	1.3 ± 1.3
I_{Fe} (%)	—	2.5 ± 0.2	0.0 ± 0.0	3.1 ± 1.3
D_J (N_J)	48.6 (24)		56.6 (24)	
$D_{X_{\max}}$ $(N_{X_{\max}})$	537.4 (329)		516.5 (329)	
D (N)	586.0 (353)		573.1 (353)	

* from $E_{\min} = 10^{17.8}$ eV.

<u>It is not possible to choose a favored scenario</u>

- Scenario 2: better X_{max} distributions and worse spectrum description
- The **differences are encompassed within the systematic uncertainties**
- In Scenario 2, photodisintegration is negligible for the LE component

  → light-to-intermediate masses (similar to the one at the sources)
- Further investigation of the Galactic-to-extragalactic transition region is necessary

Effect of the systematic uncertainties

The systematic uncertainty effect is tested in the Scenario 2

Experimental systematic uncertainties:

Systematic uncertainties from models:

Effect of the uncertainties on the predicted total fluxes and on the partial contributions from different mass groups

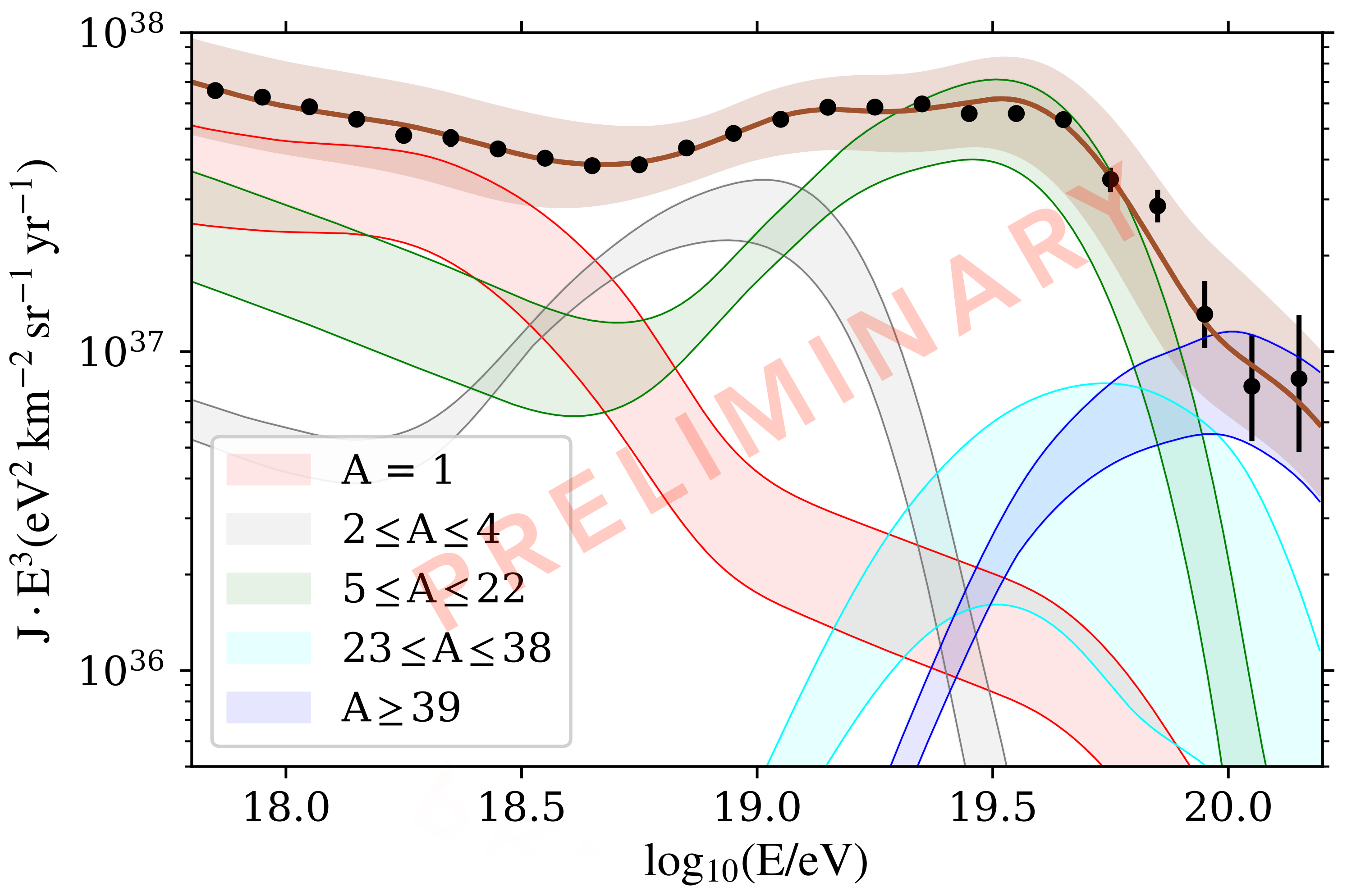

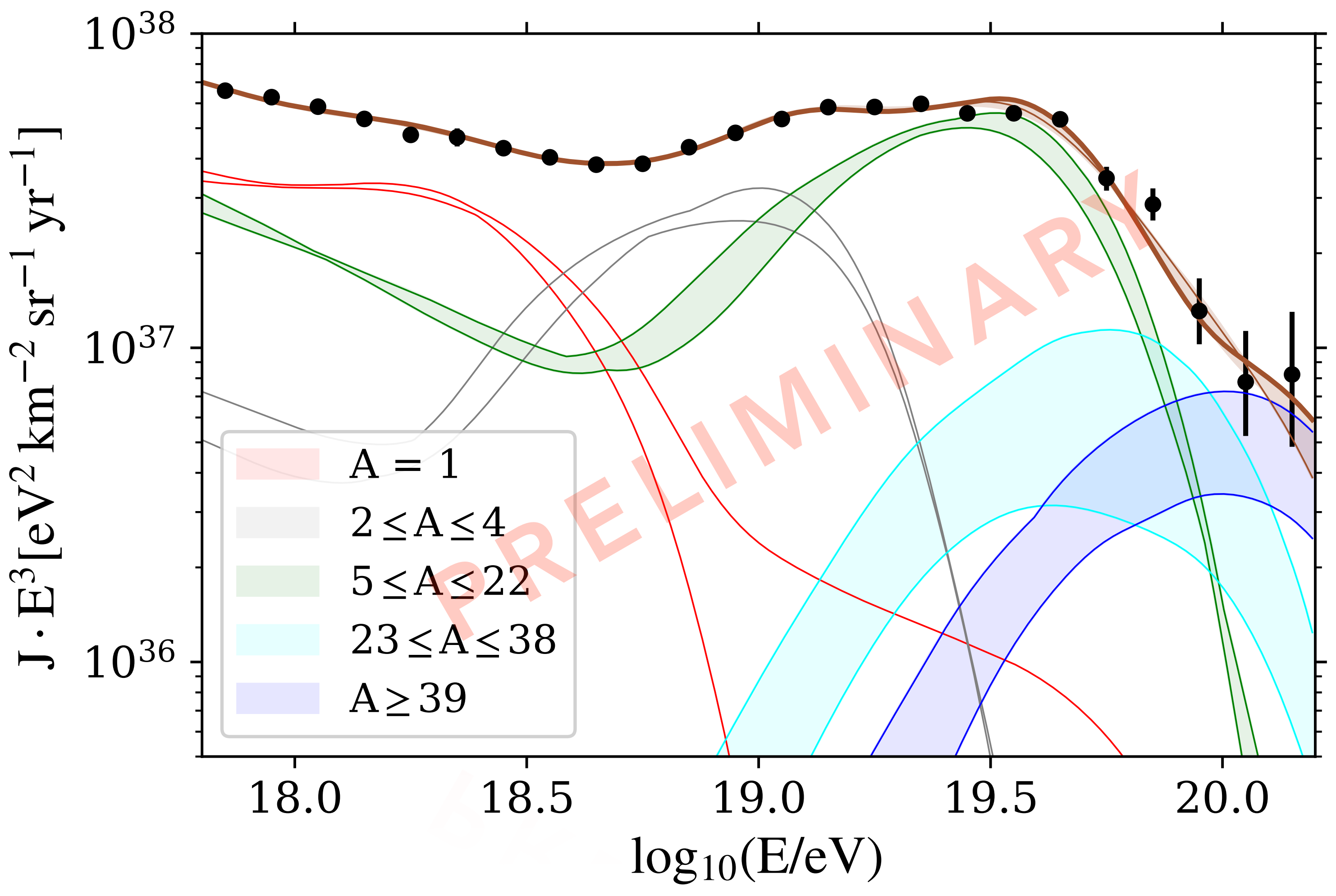

- The **dominant effect** is the one from the **experimental uncertainties** (mainly from the X_{max} scale)
- The **systematic uncertainties do not spoil our conclusions** in the reference scenarios

Cosmological evolution of sources

- Three alternative models for the **evolution of the source emissivity, parameterized as** $\propto (1+z)^m$
  → m=-3, m=+3, m=+5 (m=0 was used in the reference scenarios)
- The behavior at z>1 has only a negligible impact on the LE component (no impact on the HE one)
- All the possible combinations have been tested

Total deviance

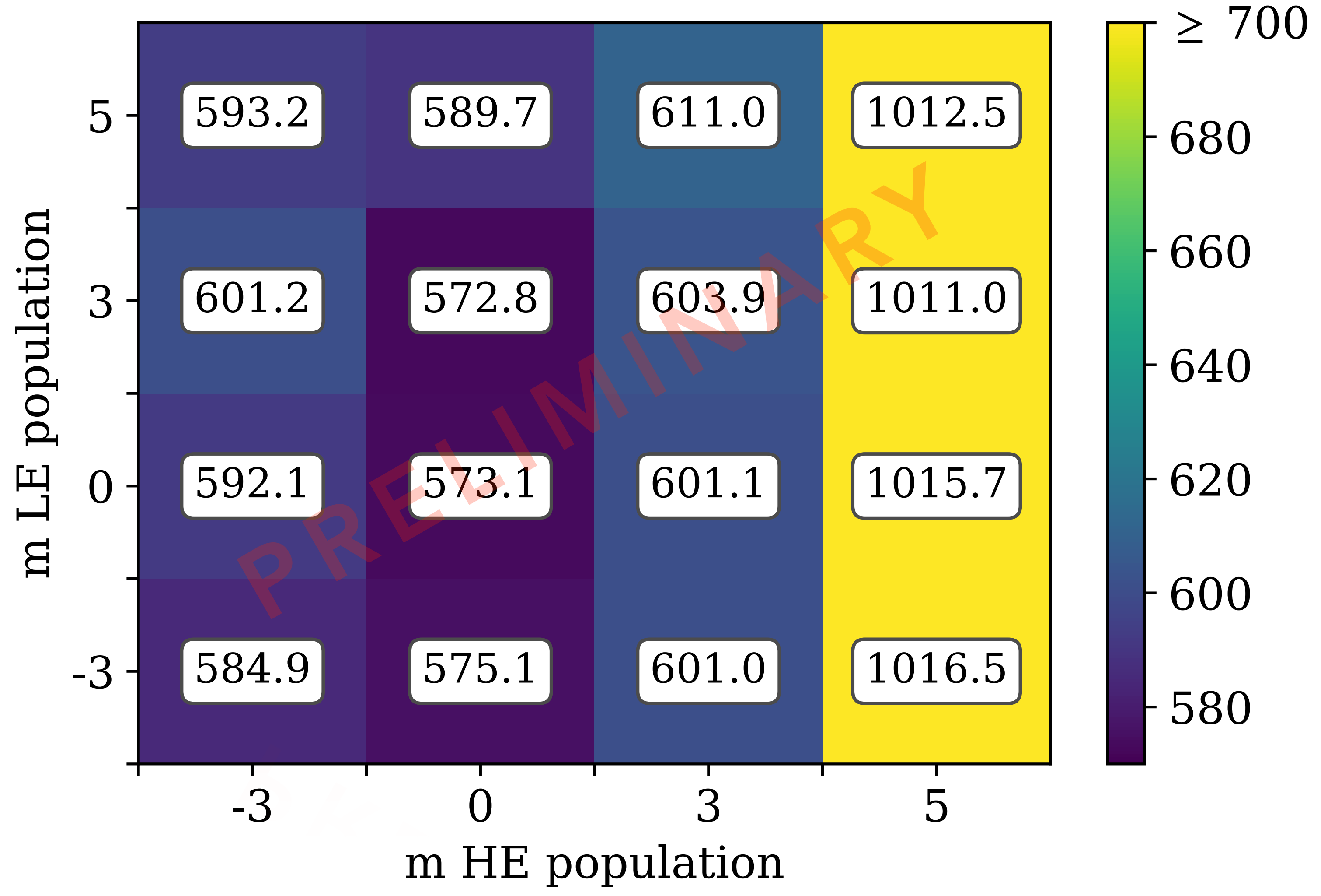

Strong source evolution for the HE is disfavored (too many secondary particles at the ankle)

Neutrinos fluxes for a strong evolution of the LE component

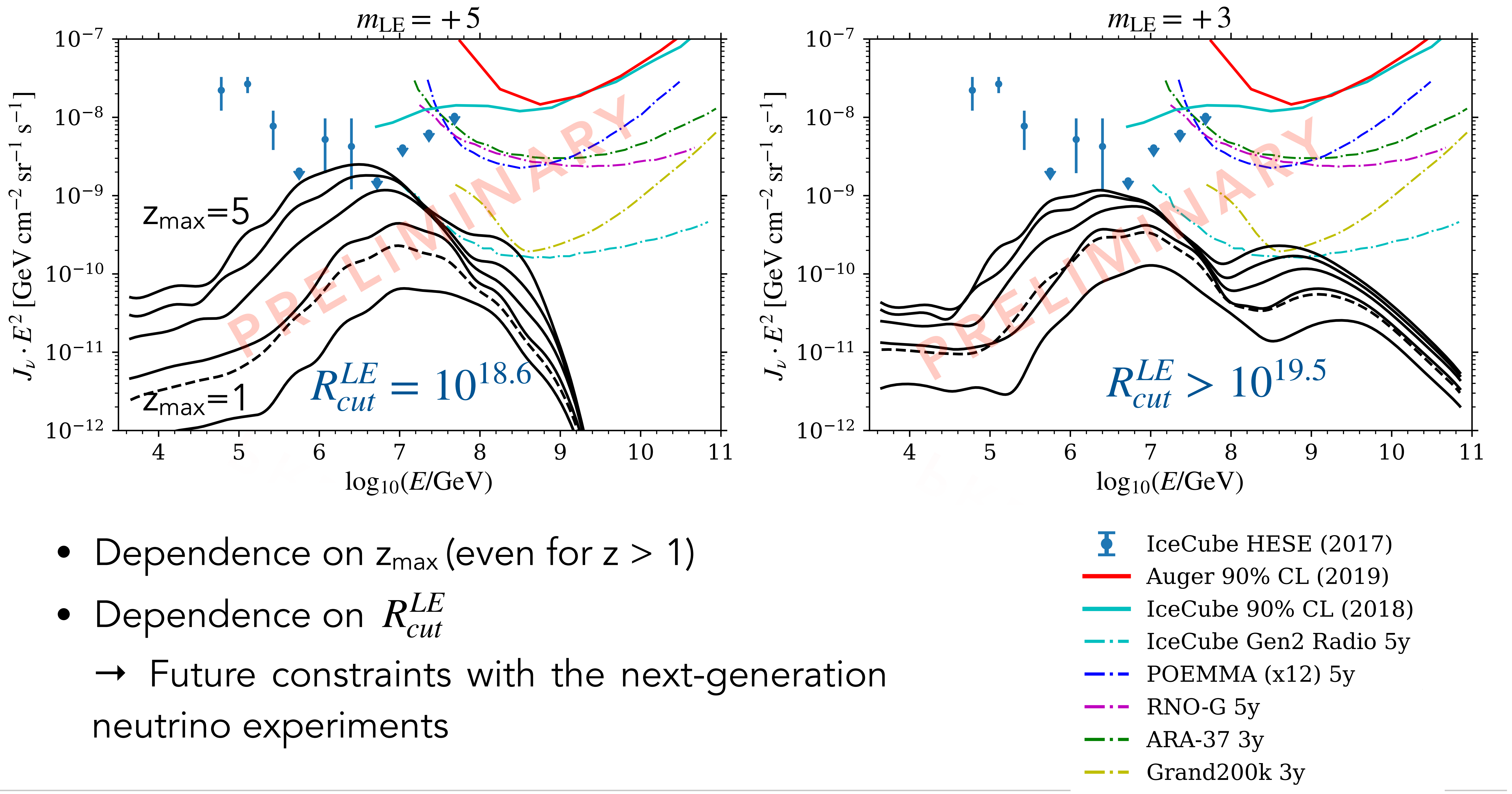

- Dependence on z_{max} (even for z > 1)
- Dependence on R_{cut}^{LE}
  → Future constraints with the next-generation neutrino experiments

Conclusions

- Simple astrophysical **model with two extragalactic components (with or without a Galactic contribution at LE)**
  - → description of the **ankle feature** at $\sim 6 \cdot 10^{18}\,\mathrm{eV}$ as the superposition of different components
  - → description of the **instep** at $\sim 10^{19}\,\mathrm{eV}$ and of the **suppression** at the highest energies
  - → **similar results** in terms of deviance **in the two scenarios**
- **Galactic component** at LE (if present) : **composition heavier than N strongly disfavored**
- The systematic uncertainties do not spoil our conclusions
- **Very strong evolution (m=5) for the HE component is excluded**
- The cosmogenic neutrino fluxes in some scenarios may reach the sensitivity of next-generation experiments

Collaboration paper about this analysis almost ready to be submitted to a journal

Outlook

- Update of the X_{max} analysis including also data from **low-energy extension of Auger** (HEAT → High-Elevation Auger Telescopes) in progress
  → *further insights on the Galactic-to-extragalactic transition region*
- Possible additional information **including arrival directions** in the fit
  → preliminary study with a combined fit above the ankle
  (presented at ICRC2021[1] and in T. Bister's poster at this conference)
- Future mass composition estimates with machine learning techniques on SD data
- Improvement of the **mass composition at the highest energies** from the detector upgrade (**AugerPrime**)
  → same analysis could be performed with *much more statistics*
  → *mass composition information at the high-energy suppression*

THANK YOU FOR YOUR ATTENTION!

[1] T. Bister for the Pierre Auger Collaboration PoS(ICRC2021)238

Back-up slides

The Pierre Auger Observatory

- **Largest observatory in the world for the detection of ultra-high-energy cosmic rays**

- Located in Argentina, close to Malargüe (~1400 m a.s.l.)
- **Ground-based experiment** detecting air-showers
- **Hybrid detection technique** (SD+FD)

~450 members from ~90 institutions in 17 countries

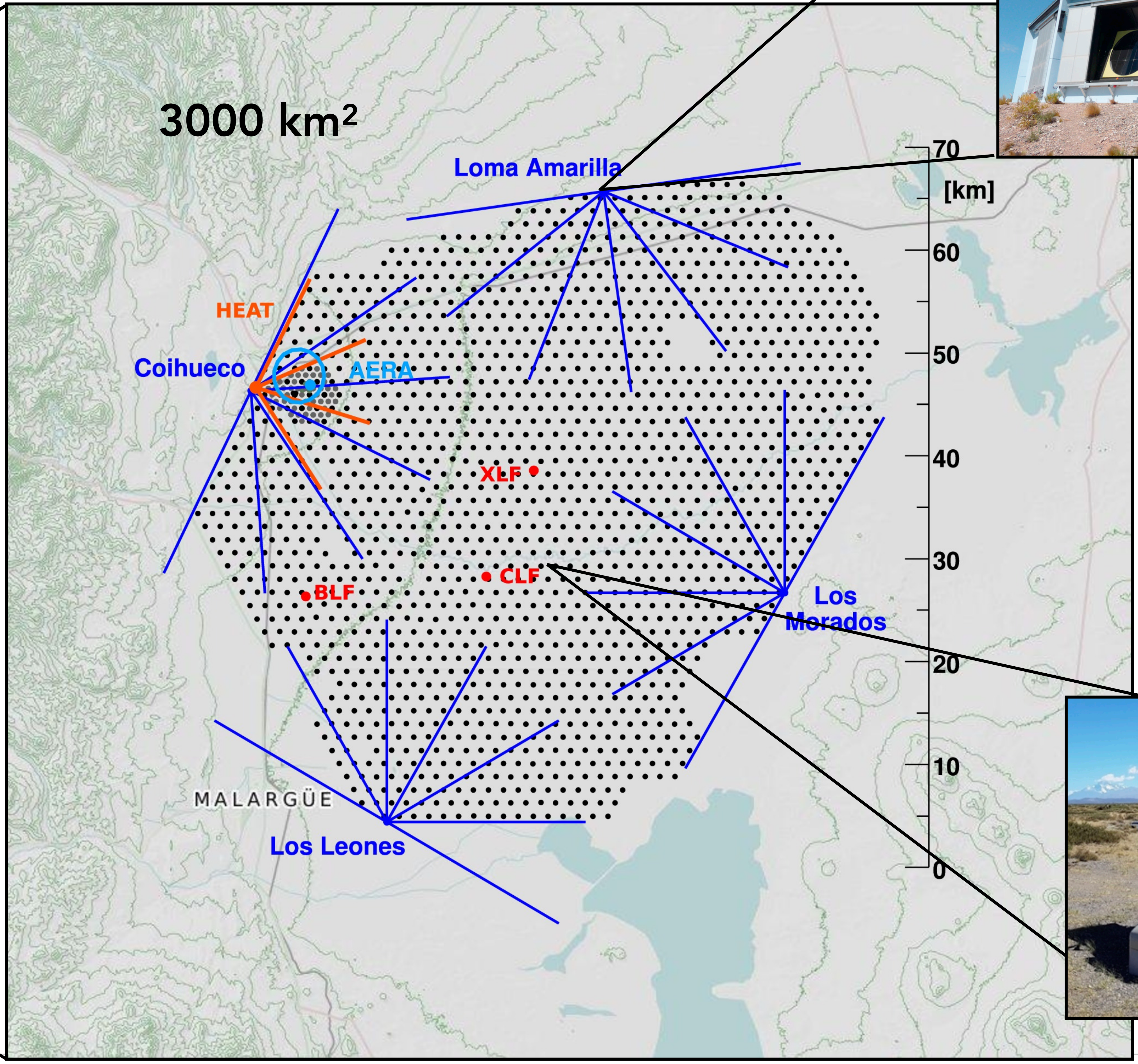

FD

SD

Effect of the systematic uncertainties from measurements

The systematic uncertainty effect is tested in the Scenario 2

Two main sources of experimental systematic uncertainties:

- **Energy scale:** $\sigma_{sys}(E)/E = 14\,\%$
- **X$_{max}$ scale:** $\sigma_{sys}(X_{max}) = 6 \div 9 \text{ g cm}^{-2}$

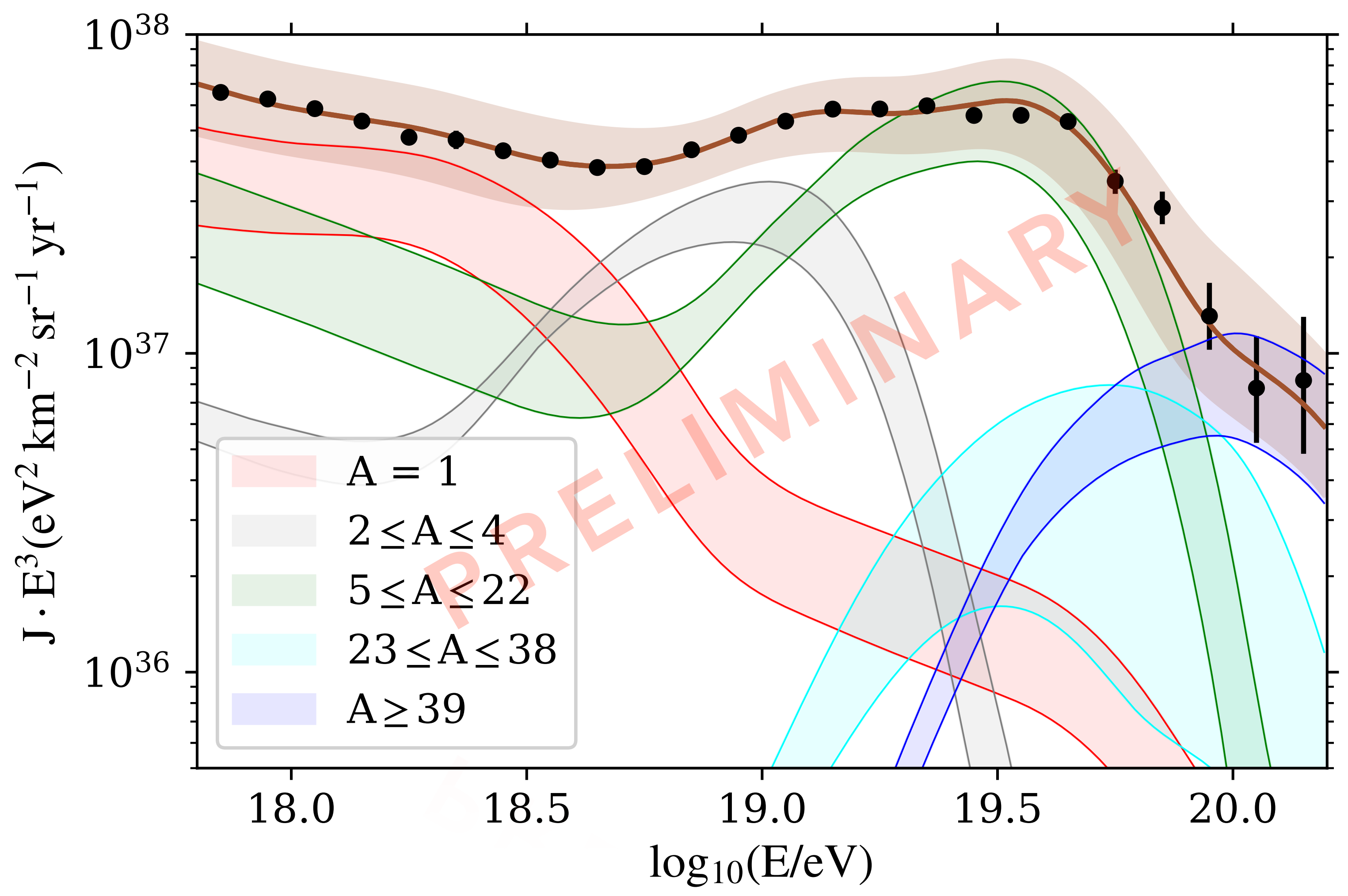

- Energy scale → shift all the energies of $\pm 1\sigma_E$ in each direction
- X$_{max}$ scale → the correlations among the energy bins are taken into account allowing for different shifts at different energies
  - ✳ The X$_{max}$ values are shifted by $a \cdot v_1(E) + b \cdot v_2(E)$
  - ✳ a, b are two additional nuisance parameters in the fit
  - ✳ A term $D_{syst} = a^2 + b^2$ has to be added to deviance

- *Large band around the total flux* due to the energy scale uncertainty → impact mainly on the estimated emissivity of sources
- The ***strongest impact*** on the predicted fluxes and on the deviance is due to the X$_{max}$ scale uncertainty

Effect of the systematic uncertainties from models

Models for propagation in the IGM and in the atmosphere

Hadronic interaction model: Sibyll2.3d / EPOS-LHC / intermediate models

- Nuisance parameter δ_{HIM} to interpolate each Gumbel parameter as
  $\alpha_{\mathrm{HIM}} = \delta_{\mathrm{HIM}} \cdot \alpha_{\mathrm{EPOS}} + (1 - \delta_{\mathrm{HIM}}) \cdot \alpha_{\mathrm{Sib}}$
- If δ_{HIM} is close to 0 → Sibyll2.3d is dominant
- If δ_{HIM} is close to 1 → EPOS-LHC is dominant

Propagation model effect:
fit repeated considering different model configurations

σ_{pd}	**T**alys, **P**SB
EBL	**G**ilmore, **D**ominguez
HIM	**E**POS-LHC, **S**ibyll2.3d, **Q**GSJetIIv4

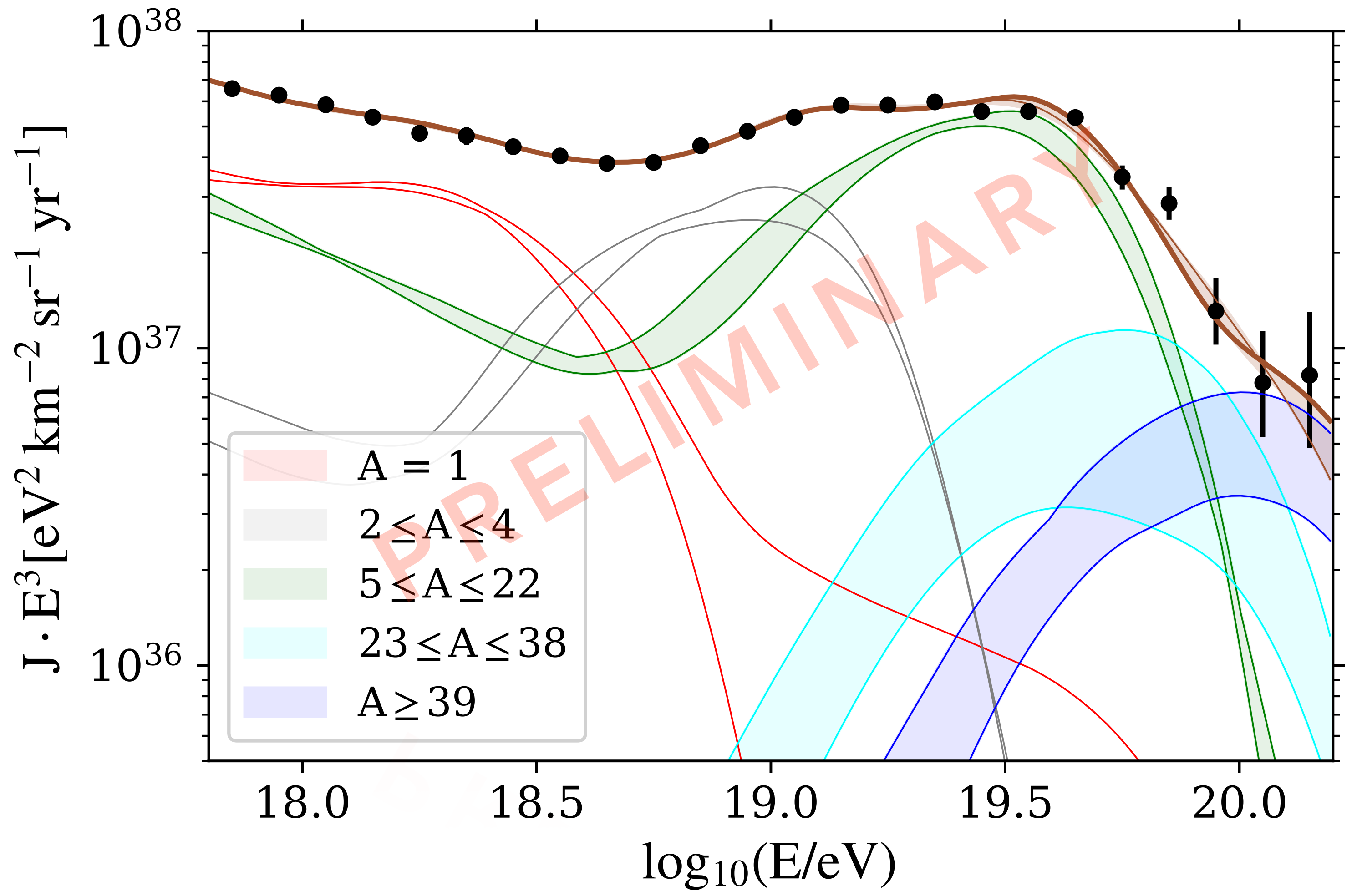

- *EPOS-LHC or models compatible with it are always preferred*
  → **HIM choice: stronger impact on D and on the predictions at Earth**
- *Propagation models*: some expected changes in the best fit parameters

The dominant effect on the the predicted fluxes and on the deviance is the one from the experimental uncertainties

Intergalactic magnetic fields

Larmor radius: $r_{\mathrm{L}} \approx 1.08 \cdot (E/\mathrm{EeV}) \cdot Z^{-1} \cdot (B_{\perp}/\mathrm{nG})^{-1}$ Mpc

Propagation theorem: the effect of intergalactic magnetic fields is negligible if the distance among sources is much lower than r_{L}

- The lowest relevant rigidity ~E/Z in our model is that of N (Z=7) at ~$10^{17.8}$ eV
- Typical distance among sources is $\lesssim 10$ Mpc

→ **magnetic fields should have $B_{\perp} \ll 10^{-11}$ G to be negligible**